Public Debt Dynamics under Ambiguity by means of Iterated Function Systems on Density Functions

Public Debt Dynamics under Ambiguity by Means of Iterated Function Systems on Density Functions

Davide La Torre[1], Simone Marsiglio[2], Franklin Mendivil[3], and Fabio Privileggi[4]

[1] *SKEMA Business School and Université Côte d'Azur, Sophia Antipolis, France. Email: davide.latorre@skema.edu.*
[2] *University of Pisa, Department of Economics and Management, Pisa, Italy. Email: simone.marsiglio@unipi.it.*
[3] *Department of Mathematics and Statistics, Acadia University, Wolfville, Canada. Email: franklin.mendivil@acadiau.ca.*
[4] *Corresponding author: Department of Economics and Statistics "Cognetti de Martiis", University of Turin, Torino, Italy. ORCID 0000-0002-8837-2006. Email: fabio.privileggi@unito.it.*

September 1, 2020

Abstract

We analyze a purely dynamic model of public debt stabilization under ambiguity. We assume that the debt to GDP ratio is described by a random variable, and thus it can be characterized by investigating the evolution of its density function through iteration function systems on mappings. Ambiguity is associated with parameter uncertainty which requires policymakers to respond to such an additional layer of uncertainty according to their ambiguity attitude. We describe ambiguity attitude through a simple heuristic rule in which policymakers adjust the available vague information (captured by the empirical distribution of the debt ratio) with a measure of their ignorance (captured by the uniform distribution). We show that such a model generates fractal-type objects that can be characterized as fixed-point solutions of iterated function systems on mappings. Ambiguity is a source of unpredictability in the long run outcome since it introduces some singularity features in the steady state distribution of the debt ratio. However, the presence of some ambiguity aversion removes such unpredictability by smoothing our the singularities in the steady state distribution.

Keywords: Ambiguity; Iterated Function Systems on Density Functions; Public Debt
JEL Classification: C61, E60, H63

1 Introduction

Uncertainty and randomness are important determinants of economic activities and macroeconomic dynamics, and thus do affect and need to be accounted for in the design of macroeconomic policy (Brock and Mirman, 1972; Rodrik, 1991; Olson and Roy, 2005; Baker et al., 2016). Recent phenomena, including the financial crisis, the climate change and the outbreak

of epidemics, have renewed the concerns about the drastic short and long run consequences of random shocks on macroeconomic outcomes, and in particular on economic growth. In order to facilitate the policymaking process, it is thus essential to understand the implications of different kinds of uncertainty on economic activities, going well beyond the typical scenario analysis employed in economic growth theory. Indeed, in the economic growth literature randomness is typically modeled by assuming that the occurrence of shocks is associated with some variable taking on some specific value with a specific probability. However, in reality parameter values are to a large extent unknown and thus policymakers need to formally take into account such a parameter uncertainty in their policy decisions (Brainard, 1967; Brock and Durlauf, 2006; Hansen and Sargent, 2007; Born and Pfeifer, 2014). How to effectively deal with such information-based uncertainty in macroeconomic modeling is still an open question but it clearly requires to deal with ambiguity. With some exception in the field of economic growth (Cozzi and Giordani, 2011), most of the attempts to address ambiguity issues focus on monetary and fiscal countercyclical policy (Karantounias, 2013; Caprioli, 2015; Hollmayr and Matthes, 2015). Our paper aims to contribute to this literature by developing a novel approach based on iteration function systems on density functions in the context of economic growth and public debt stabilization. Unlike extant works which focus on how optimal policymaking is affected by ambiguity, we concentrate on a purely dynamic setting in order to characterize the policymaker's reaction to ambiguity by the means of a heuristic rule which allows us to identify the implications of ambiguity attitude on the steady state outcome and to investigate its eventual fractal properties.

Our paper is therefore related to the literature on the fractal nature of the steady state in macroeconomic models, which mainly focuses on economic growth setups. Several works analyze how random shocks in economic growth models may eventually generate trajectories converging to invariant measures supported on fractal sets, and thus how their steady states can thus be characterized in terms of their fractal features (Montrucchio and Privileggi, 1999; Mitra et al., 2003). Most of the papers focus on one- and multi-sector growth frameworks driven by different forms of capital accumulation in which stochasticity affects productivity (La Torre et al., 2011, 2015, 2018b), while only few are those in which randomness influences some other macroeconomic variable, like polluting emissions (Privileggi and Marsiglio, 2013; La Torre et al., 2018a). Such studies show that the support of the invariant measure may take the form of different fractal sets, including the famous Cantor set, the Sierpinski gasket and the Barnsley's fern. All these works assume that uncertainty is entirely captured by the occurrence of a limited number of alternative scenarios, each of which takes place with a known probability, and thus cannot analyze the implications of ambiguity on steady state outcomes.

The works on ambiguity go back to Ellsberg (1961) who firstly shows that people tend to neatly distinguish between known (*i.e.*, unambiguous or objective) probabilities and unknown (*i.e.,* ambiguous or subjective) probabilities. The definition of ambiguity is not unique and different types of ambiguities have been considered in literature (see Camerer and Weber, 1992; and Etner et al., 2012, for concise surveys), but in general terms *"ambiguity is uncertainty about probability created by missing information that is relevant and could be known"* (Frisch and Baron, 1988). Agents' reaction to such an ambiguity is referred to as ambiguity attitude, which, as shown in experimental studies, may change from aversion to attraction (Ghirardato et al., 2004). Different types of ambiguity attitude may play an important role in driving macroeconomic dynamics, but to the best of our knowledge the only attempt to analyze its consequences in an economic growth setup is represented by Cozzi and Giordani's (2011), which introduces ambiguity in a Schumpeterian growth framework to describe the innovation process showing that ambiguity aversion plays a detrimental role on economic performance. We

contribute to this literature by analyzing the implications of ambiguity and ambiguity attitude on the steady state of stochastic growth models by focusing in particular on their implications for public debt.

Specifically, different from extant literature which focuses on traditional economic growth models, we embed a simplified growth setup into a model of public debt stabilization to investigate the impact of ambiguity on debt dynamics. We analyze a purely dynamic setting in which fiscal policy instruments are determined through a rule of thumb such that the debt dynamics is exogenously given and generated through an iterated function system on density functions. The level of public debt is no longer described by a number but, instead, it is modeled through a random variable and then by means of its density function. Public debt can be modeled as a random variable to take into account the uncertainty associated with the formation of expectations in modern economies, which by determining the cost of borrowing crucially determines the evolution of debt. Different from previous works in which the noise is modeled by a Bernoulli process (see La Torre et al., 2015, 2018b), we do not make any specific assumption on the underlying stochastic process and thus our results are more widely applicable. Apart from the uncertainty associated with the formation of expectations in the financial market which per se makes public debt a random variable, we consider an additional layer of uncertainty related to vague information about the relevant parameter values. This introduces ambiguity in the sense that policymakers need to develop some subjective assessments to forecast the values of such parameters. This implies that its empirical distribution provides only partially reliable information regarding the evolution of public debt, and thus policymakers may need to respond to this additional layer of uncertainty according to their ambiguity attitude. We describe ambiguity attitude through a simple heuristic rule in which policymakers adjust the empirical distribution of the debt ratio with a a measure of their ignorance, captured by the uniform distribution. We show that ambiguity is a source of unpredictability since it introduces some singularity features in the steady state distribution of the debt ratio and as such the equilibrium outcome is extremely uncertain. However, the presence of some ambiguity aversion removes such unpredictability by smoothing out the singularities in the steady state distribution reducing thus the degree of uncertainty associated with the equilibrium outcome. Therefore, ambiguity aversion plays an important role since it allows to reduce the variability in the evolution of public debt.

The paper is organized as follows. Section 2 discusses the mathematical tools that we will employ in our analysis, presenting the theories of generalized fractal transforms, of iterated function systems on maps and density functions. Section 3 presents our debt stabilization model in its simplest form (in which ambiguity is not taken into account) to clarify how the debt dynamics allows us to infer the evolution of its density. Section 4 introduces ambiguity related to the fact that parameter values are only vaguely known, showing how the presence of ambiguity affects the evolution of the density of the public debt. Section 5 considers policymakers' response to ambiguity formalized through a simple rule in which the empirical and the uniform distribution of the public debt are combined together to determine the evolution of the density of the public debt. Section 6 presents some numerical simulations to exemplify the implications of our modeling approach and the dynamic evolution of the distribution of the public debt under different circumstances. Section 7 as usual concludes and proposes directions for future research.

2 Mathematical Preliminaries

We now discuss the main mathematical tool that we will later use in our analysis, that is iterated function systems on density functions. We will take for granted basic concepts on iterated function systems and fractal attractors (see, among others, La Torre et al., 2015, for a concise review of these notions; a more formal presentation can be found in Kunze et al., 2012), and we will focus on the theory of generalized fractal transforms, and the theory of iterated function systems on maps and how the operator of iterated function systems on maps works on the set of density functions.

2.1 Generalized Fractal Transforms

Let (X, d) be a metric space. The action of a generalized fractal transform (GFT) $T : X \to X$ on an element u of the complete metric space (X, d) is described by the following steps: it produces a set of N spatially-contracted copies of u; then it modifies the values of these copies by means of a suitable range-mapping; finally, it recombines them using an appropriate operator in order to get the element $v \in X$, $v = Tu$ (Barnsley, 1989; Kunze et al., 2012). In all these cases, under appropriate conditions, the fractal transform T is a contraction and thus Banach's fixed point theorem guarantees the existence of a unique fixed point $\bar{u} = T\bar{u}$.

Definition 1. *(Contraction mapping) [Banach, 1922] Let $T : X \to X$ be a mapping on a complete metric space (X, d). Then T is said to be contractive if there exists a constant $c \in [0, 1)$ such that $d(Tx, Ty) \leq cd(x, y)$ for all $x, y \in X$.*

The *contraction factor* of T is the smallest such $c \in [0, 1)$ for which the above inequality holds true. We now come to what is perhaps the most famous theorem regarding contraction maps on metric spaces and certainly central to fractal-based methods.

Theorem 1. *(Banach's Fixed Point Theorem) [Banach, 1922] Let $T : X \to X$ be a contraction mapping on X with contraction factor $c \in [0, 1)$ mapping on X. Then,*

1. *There exists a unique element $\bar{x} \in X$, the fixed point of T, for which $T\bar{x} = \bar{x}$.*
2. *Given any $x_0 \in X$, if we form the iteration sequence $x_{n+1} = T(x_n)$, then $x_n \to \bar{x}$, i.e., $d(x_n, \bar{x}) \to 0$ as $n \to \infty$. In other words, the fixed point $\bar{x}$ is globally attractive.*

Theorem 1 states that, under the contractivity condition, there exists a unique fixed point of T, which any orbit in X is converging to. When the operator T is not a contraction but it is only a Lipschitz map (that is, c is not necessarily less than 1) we can still prove the following result.

Corollary 1. *Let $T : X \to X$ be a Lipschitz mapping on X with Lipschitz factor $C \geq 0$ and $x_{n+1} = Tx_n$ be the orbit generated from $x_0 \in X$. If $x_n \to \bar{x}$, then $\bar{x}$ is a fixed point of T.*

Proof. The proof follows from the following sequence of calculations:

$$\begin{aligned} d(\bar{x}, T\bar{x}) &\leq d(\bar{x}, x_{n+1}) + d(x_{n+1}, T\bar{x}) \\ &= d(\bar{x}, x_{n+1}) + d(Tx_n, T\bar{x}) \\ &\leq d(\bar{x}, x_{n+1}) + Cd(x_n, \bar{x}) \end{aligned}$$

and, by taking the limit when $n \to +\infty$, we get that $d(\bar{x}, T\bar{x}) = 0$, that is $\bar{x}$ is a fixed point of T. ■

Corollary 1 states that, in the absence of the contractivity condition, the uniqueness of the fixed point of T cannot be ensured, but nevertheless the limit point of any converging orbit in X is a fixed point of T.

2.2 Iterated Function Systems on Mappings

We now focus on the method of iterated function systems on mappings (IFSM), as formulated in Forte and Vrscay (1995). IFSMs extend the classical notion of iterated function systems (IFS) to the case of space of functions (Kunze et al., 2012) and can be used to generate integrable "fractal" functions. An IFSM can be used to approximate a given element u of $L^p([0,1])$, with $p \geq 1$. As usual L^p is equipped with the $\|\cdot\|_p$ norm and then the induced distance d_p. In the sequel, using the notation presented earlier, we define $X = L^p([0,1])$. The ingredients of an N-map IFSM on $L^p([0,1])$ are:

1. a set of N contractive mappings $w = \{w_1, w_2, \ldots, w_N\}$, $w_i(x) : [0,1] \to [0,1]$, most often affine in form:

$$w_i(x) = s_i x + a_i, \qquad 0 \leq |s_i| < 1, \qquad i = 1, 2, \ldots, N; \tag{1}$$

2. a set of associated functions—the greyscale maps—$\phi = \{\phi_1, \phi_2, \ldots, \phi_N\}$, $\phi_i : \mathbb{R} \to \mathbb{R}$. Affine maps are usually employed:

$$\phi_i(y) = \alpha_i y + \beta_i. \tag{2}$$

Associated with the N-map IFSM (w, ϕ) is the *fractal transform* operator T, the action of which on a function $u \in X$ is given by:

$$(Tu)(x) = {\sum_{i=1}^{N}}' \phi_i\left(u\left(w_i^{-1}(x)\right)\right), \tag{3}$$

where the prime means that the sum operates only on those terms for which w_i^{-1} is defined. The following result in Proposition 1 states that T is a Lipschitz map on $L^p([0,1])$.

Proposition 1. *[Forte and Vrscay, 1995] For any $p \geq 1$ we have that $T : L^p([0,1]) \to L^p([0,1])$ and for any $u, v \in L^p([0,1])$ we have:*

$$d_p(Tu, Tv) \leq C d_p(u, v)$$

where:

$$C = \sum_{i=1}^{N} s_i^{\frac{1}{p}} |\alpha_i|.$$

Corollary 2. *Suppose that $C = \sum_{i=1}^{N} s_i^{\frac{1}{p}} |\alpha_i| < 1$. Then T has a unique fixed point $\bar{u} \in L^p([0,1])$ and, for any $u_0 \in L^p$, the orbit generated $u_{n+1} = Tu_n$ converges to $\bar{u}$ whenever $n \to +\infty$.*

The above corollary states that if $\sum_{i=1}^{N} s_i^{\frac{1}{p}} |\alpha_i| < 1$ then the IFSM operator is a contraction on L^p and hence it has a unique fixed point $\bar{u}$ that is attracting any orbit $T^n u_0$ generated starting from any point $u_0 \in L^p$. Notice that if $\bar{u} \in L^p$, $p \geq 1$, then $\bar{u} \in L^q$ for any $1 \leq q \leq p$.

2.3 Iterated Function Systems on Density Functions

We are now ready to show that, under certain hypotheses, an IFSM operator is a contraction with respect to the usual norm introduced into the space of density functions.

Definition 2. *For any $p \geq 1$, the space of* density functions U^p *is defined as follows:*

$$U^p = \left\{ u : [0,1] \to \mathbb{R}, u \in L^p([0,1]), u(x) \geq 0 \ \forall x \in [0,1], \int_{[0,1]} u(x)\,\mathrm{dx} = 1 \right\},$$

where dx *denotes the Lebesgue measure on* $[0,1]$.

Let us notice that $U^p \subseteq U^q$ for any $1 \leq q \leq p$. Now we show that under certain conditions the IFSM operator T earlier defined is a contraction mapping on U. It is trivial to prove that $U \subset L^p([0,1])$ as defined earlier.

Proposition 2. *The space U^p is complete with respect to the usual d_p norm.*

Proof. The proof of this result follows from the following two facts: if f_n is a converging sequence of (a.e.) positive functions in L^p to f then there exists a subsequence that is a.e. pointwise converging to f and this implies the positivity of f. Furthermore, if f_n has integral over $[0,1]$ equal to 1 then the L^p limit also possesses this property. ■

In the rest of the paper we suppose that the non-overlapping property holds, which means that the following assumption on the maps w_i is satisfied.

A. 1. *The maps w_i, for $i = 1, \ldots, N$, satisfy the following conditions:*

i) $\cup_{i=1}^{N} w_i[0,1] = [0,1]$,

ii) $\mathrm{dx}(w_i([0,1]) \cap w_j([0,1])) = 0$ *for any $i \neq j$, where* dx *denotes the Lebesgue density on* $[0,1]$.

Proposition 3. *Under Assumption A.1 suppose that the following conditions are satisfied:*

i) $\alpha_i, \beta_i \in \mathbb{R}_+$ *for all* $i = 1...N$,

ii) $\sum_{i=1}^{N} s_i(\alpha_i + \beta_i) = 1$.

Then the operator T defined as:

$$(Tu)(x) = \sum_{i=1}^{N} {}'\phi_i\left(u\left(w_i^{-1}(x)\right)\right), \tag{4}$$

maps U into itself. Furthermore, if:

$$\sum_{i=1}^{N} s_i^{\frac{1}{p}} \alpha_i < 1 \tag{5}$$

then T is a contraction over U. This implies that T has a unique fixed point $\bar{u}$ that is also a global attractor for any sequence taking the form:

$$u_{n+1} = Tu_n$$

for any initial condition $u_0 \in U^p$.

Proof. The only property that needs to be proved is that T maps U^p into itself. From the hypotheses on the signs of α_i, β_i it follows that Tu is positive whenever u is positive. To show that the integral is one, let us do some computations:

$$\begin{aligned}
\int_{[0,1]} (Tu)(x)\,dx &= \int_{[0,1]} \sum_{i=1}^{N} {}'\phi_i\left(u\left(w_i^{-1}(x)\right)\right) dx \\
&= \sum_{i=1}^{N} \int_{[0,1]} {}'\phi_i\left(u\left(w_i^{-1}(x)\right)\right) dx \\
&= \sum_{i=1}^{N} \int_{w_i([0,1])} \phi_i\left(u\left(w_i^{-1}(x)\right)\right) dx \\
&= \sum_{i=1}^{N} s_i \int_{[0,1]} \phi_i\left(u(x)\right) dx \\
&= \sum_{i=1}^{N} s_i \left[\alpha_i \int_{[0,1]} u(x)\,dx + \beta_i \int_{[0,1]} dx\right] = 1
\end{aligned}$$

■

Proposition 3 states that the operator T maps U^p into itself and the fixed point equation $Tu = u$ has a unique solution that is attracting any orbit $T^n u_0$ for any $u_0 \in U^p$. In the sequel we will suppose, for simplicity, $p = 2$ and we denote U^2 by U. All the results can be easily extended to the case $p \neq 2$.

3 The Benchmark Model

We now present our benchmark model abstracting completely from ambiguity, which will be introduced later. We analyze a purely dynamic model of economic growth and public debt, along the lines of La Torre and Marsiglio (2019). We consider a small open economy in which the interest rate on international borrowing is exogenously given and public debt is used to finance public spending. Households consume completely their disposable income: $C_t = \left[1 - \tau\left(\frac{B_t}{Y_t}\right)\right] Y_t$, where C_t denotes consumption, Y_t income, B_t public debt, and $\tau\left(\frac{B_t}{Y_t}\right) \in (0,1)$ is the tax rate, which is an increasing function of the debt-to-GDP ratio. The tax revenue $R_t = \tau\left(\frac{B_t}{Y_t}\right) Y_t$ is entirely devoted to repay public debt. Income grows exogenously at the rate $\gamma > 0$ as follows: $Y_{t+1} = (1+\gamma) Y_t$. An exogenous share of such an income, $0 < g < 1$, is devoted to public spending, $G_t = gY_t$, which is entirely financed via debt accumulation. Public debt accumulation increases with interest payments, $(1+r) B_t$, and public spending, gY_t, while it decreases with the tax revenue, as follows: $B_{t+1} = (1+r) B_t + G_t - R_t$. We assume that the tax rate is a linear function of debt-to-GDP ratio as follows: $\tau\left(\frac{B_t}{Y_t}\right) = \tau \frac{B_t}{Y_t}$ where $0 < \tau \leq 1$ is a scale parameter. This assumption is consistent with the results in La Torre and Marsiglio (2019), which show that if policymakers determine optimally the tax rate in order to minimize the social costs associated with debt accumulation they will find it optimal to set the tax rate proportionally to the debt-to-GDP ratio. We also assume that $0 \leq B_t \leq Y_t$, such that the debt-to-GDP ratio is bounded between zero and one, that is $\frac{B_t}{Y_t} \in [0,1]$, which simply means that we normalize the values of the debt ratio to represent with $\frac{B_t}{Y_t} = 1$ its maximum (unsustainable) level.

Given the dynamic equations for income and debt, it is straightforward to derive the law of motion of the debt-to-GDP ratio, $x_t = \frac{B_t}{Y_t}$, which reads as follows:

$$x_{t+1} = w(x_t) \tag{6}$$

where $w : [0,1] \to \left[\frac{g}{1+\gamma}, \frac{1+r-\tau+g}{1+\gamma}\right]$ is defined as:

$$w(x) = \frac{1+r-\tau}{1+\gamma}x + \frac{g}{1+\gamma}. \tag{7}$$

Similar to La Torre and Marsiglio (2019), equations (6) and (7) suggest that, intuitively, a higher growth rate reduces the accumulation of the debt ratio by increasing the amount of resources available to debt repayment activities; a higher interest rate increases the accumulation of the debt ratio by increasing interest payments; a higher income share of public spending increases the accumulation of the debt ratio by deteriorating the public budget balance position; a higher tax coefficient reduces the accumulation of the debt ratio by improving the public budget balance position. If the public budget balance were in equilibrium, $G_t = R_t$, then the evolution of public debt would depend only on the gap between the interest and the growth rates, and in particular the debt ratio would tend to increase (decrease) over time whenever the interest rate is larger (smaller) than the growth rate. Disequilibrium in the public budget balance position introduces a wedge between the growth and interest rate gap and its impact on the debt ratio.

If fiscal policy instruments (*i.e.*, the tax rate parameter, τ, and the government spending to GDP ratio, g) are appropriately chosen in order to stabilize public debt, then the following parameter restriction will apply $0 < \frac{1+r-\tau+g}{1+\gamma} < 1$, ensuring that in the long run the public debt will converge to a positive finite value. Therefore, in the following we shall assume that:

$$0 \leq \frac{1+r-\tau}{1+\gamma} < \frac{1+r-\tau+g}{1+\gamma} \leq 1, \tag{8}$$

which implies that the function w is a contraction map transforming $[0,1]$ into (a subset of) itself. In this case we can interpret w as a (unique) map of the type defined by (1) with $s = \frac{1+r-\tau}{1+\gamma}$ and $a = \frac{g}{1+\gamma}$. In such a specific framework, (6) describes a very simple dynamical system which is globally convergent to the fixed point:

$$\bar{x} = \frac{g}{\gamma - r + \tau}, \tag{9}$$

which, under condition (8), is interior to the interval $[0,1]$ because $0 < g < 1$. Therefore, under the assumption of effectiveness in the debt stabilization policy instruments, in the long run the public debt-to-GDP ratio will converge to a strictly positive level, which intuitively increases with the government spending to GDP ratio and the interest rate on borrowing, while it decreases with the growth rate and the tax rate parameters.

Thus far we have simply assumed that there is no uncertainty and thus that the debt ratio is a completely deterministic variable. However, the international financial market is characterized by a large degree of randomness, and as the expectations within the market change (driven by the financial agents' speculative or hedging motives) the interest rate may change as well and thus the debt ratio turns out to be stochastic. In light of such expectations-driven changes in the interest rate, we now suppose that the debt ratio is no longer deterministic but instead a random variable with an associated density function u_t. Different from extant works which assume that the noise is driven by a Bernoulli process we do not make any specific assumption about the process underlying such a stochasticity, thus our following discussion and results

apply in general terms. If x_t is a random variable depending on the underlying probability space and u_t its density, then, for any $\theta_1 \leq \theta_2$, we can perform the following calculations:

$$\begin{aligned}\int_{\theta_1}^{\theta_2} u_{t+1}(y)\,\mathrm{dy} &= \Pr(\theta_1 \leq x_{t+1} \leq \theta_2)\\ &= \Pr\left(\theta_1 \leq \frac{1+r-\tau}{1+\gamma}x_t + \frac{g}{1+\gamma} \leq \theta_2\right)\\ &= \Pr\left(\theta_1 - \frac{g}{1+\gamma} \leq \frac{1+r-\tau}{1+\gamma}x_t \leq \theta_2 - \frac{g}{1+\gamma}\right)\\ &= \Pr\left(\frac{(1+\gamma)\theta_1 - g}{1+r-\tau} \leq x_t \leq \frac{(1+\gamma)\theta_2 - g}{1+r-\tau}\right)\\ &= \int_{\frac{(1+\gamma)\theta_1-g}{1+r-\tau}}^{\frac{(1+\gamma)\theta_2-g}{1+r-\tau}} u_t(y)\,\mathrm{dy}\,. \end{aligned} \tag{10}$$

If we set:

$$y = w^{-1}(z) = \frac{(1+\gamma)z - g}{1+r-\tau} \qquad \Longleftrightarrow \qquad z = w(y) = \frac{1+r-\tau}{1+\gamma}y + \frac{g}{1+\gamma},$$

the integral on the LHS of (10) boils down to:

$$\begin{aligned}\int_{\theta_1}^{\theta_2} u_{t+1}(y)\,\mathrm{dy} &= \int_{\frac{(1+\gamma)\theta_1-g}{1+r-\tau}}^{\frac{(1+\gamma)\theta_2-g}{1+r-\tau}} u_t(y)\,\mathrm{dy} = \int_{w^{-1}(\theta_1)}^{w^{-1}(\theta_2)} u_t(y)\,\mathrm{dy} = \int_{\theta_1}^{\theta_2} u_t\left[w^{-1}(z)\right]\left(w^{-1}\right)'(z)\,\mathrm{dz}\\ &= \frac{1+\gamma}{1+r-\tau}\int_{\theta_1}^{\theta_2} u_t\left[w^{-1}(z)\right]\mathrm{dz}\,.\end{aligned}$$

Since this is true for any pair θ_1, θ_2 such that $\theta_1 \leq \theta_2$, we can summarize the temporal evolution of the density u_t of x_t by means of the following operator $T^* : U \to U$ defined as:

$$u_{t+1} = T^* u_t = \frac{1+\gamma}{1+r-\tau}u_t \circ w^{-1}, \tag{11}$$

resembling an embryo of the more general operator T defined in (4) whose constituents are the map $w(x) = sx + a$ with $s = \frac{1+r-\tau}{1+\gamma}$ and $a = \frac{g}{1+\gamma}$, together with a greyscale map $\phi(y) = \alpha y + \beta$ of the type defined by (2) with $\alpha = \frac{1+\gamma}{1+r-\tau}$ and $\beta = 0$. The above equation (11) states that at each iteration, the density of the debt ratio at time $t+1$ is obtained as a modified (distorted) copy of the empirical distribution of the debt ratio at time t, u_t, since the composition with the inverse of w_i times the greyscale parameter α allows for possible shifting and rescaling of the density function. Specifically, the composition of the density with the inverse of w_i shrinks its support while coefficient $\alpha = \frac{1+\gamma}{1+r-\tau}$ rescales the marginal densities.

Note that the operator in (11), although it maps U into itself, unfortunately it is not a contraction over U, as it does not satisfy condition (5) in Proposition 3, because under our parameter restriction (8) the following holds true:

$$s^{\frac{1}{2}}\alpha = \left(\frac{1+r-\tau}{1+\gamma}\right)^{\frac{1}{2}}\frac{1+\gamma}{1+r-\tau}\left(\frac{1+\gamma}{1+r-\tau}\right)^{\frac{1}{2}} = \left(\frac{1+\gamma}{1+r-\tau}\right)^{\frac{1}{2}} > 1.$$

However, despite the absence of contractivity, the fixed point equation;

$$\bar{u} = T^*\bar{u} = \frac{1+\gamma}{1+r-\tau}\bar{u} \circ w^{-1}, \tag{12}$$

has a solution $\bar{u}$ in some extended sense. In fact, the Dirac distribution concentrated at the fixed point $\bar{x}$ of the map w defined in (9), which we will denote by $\delta_{\frac{g}{\gamma-r+\tau}}(x)$, is the fixed point of (12), but unfortunately, $\delta_{\frac{g}{\gamma-r+\tau}}(x)$ is not an element of U. This can be proved more formally by transforming the operator in (12) into its equivalent counterpart in the space of cumulative distribution functions. Let us define the cumulative distribution function associated to u as $F(x) = \int_0^x u(v)\,\mathrm{dv}$. Simple calculations show that:

$$\begin{aligned} F_{t+1}(x) &= \int_0^x u_{t+1}(v)\,\mathrm{dv} = \int_0^x T^* u_t(v)\,\mathrm{dv} = \int_0^x \frac{1+\gamma}{1+r-\tau} u_t\left[w^{-1}(v)\right]\mathrm{dv} \\ &= \frac{1+\gamma}{1+r-\tau}\int_{w^{-1}(0)}^{w^{-1}(x)} u_t(z)\,w'(v)\,\mathrm{dz} = \frac{1+\gamma}{1+r-\tau}\left(\frac{1+r-\tau}{1+\gamma}\right)\int_0^{w^{-1}(x)} u_t(z)\,\mathrm{dz} \\ &= F_t\left[w^{-1}(x)\right], \end{aligned} \tag{13}$$

where in the third equality we use the definition in (11), while the fifth equality follows from $w'(v) \equiv \frac{1+r-\tau}{1+\gamma}$ and the fact that $w^{-1}(0) \leq 0$, so that the interval $[w^{-1}(0), 0]$ lies outside the support of u_t. Because $w(x) = sx + a$ is a contraction with (constant) slope $s = \frac{1+r-\tau}{1+\gamma} < 1$ the image set $w([0,1])$ is a proper subset of $[0,1]$, $w([0,1]) \subset [0,1]$, which collapses to the fixed point $\bar{x} = \frac{g}{\gamma-r+\tau}$ defined in (9) as $t \to \infty$. Therefore, after each iteration of operator T^* in (11), the support of the marginal density u_t keeps shrinking as t increases, which, in turn, implies that the associated cumulative distribution function F_t becomes steeper on such a support as t increases, eventually collapsing to the Dirac distribution $\delta_{\frac{g}{\gamma-r+\tau}}(x)$ defined as:

$$\bar{F}(x) = \begin{cases} 0 & \text{if } 0 \leq x < \dfrac{g}{\gamma-r+\tau} \\ 1 & \text{if } \dfrac{g}{\gamma-r+\tau} \leq x < 1, \end{cases}$$

which is the unique fixed point of the equation $F(x) = F[w^{-1}(x)]$. To see that $\bar{F}$ is unique note that the support of the marginal density u_t along the trajectory generated by system (11) converges to the single point $\bar{x}$ defined in (9), so that as $t \to \infty$ the whole probability must necessarily be concentrated on the point $\bar{x}$ itself. In such a benchmark case in which the only source of uncertainty is the randomness in the financial market's expectations, then the model's equilibrium coincides with the deterministic steady state, such that the long run value of the debt-to-GDP ratio can be perfectly predicted.

Besides the benchmark model defined by operator T^* in (11) under the parameter restriction (8), which guarantees the contractivity condition, it is worth to explore the model's behavior in the specific case in which $g = 0$ and $\tau = r - \gamma$ (under the assumption that $r > \gamma$). Such a special case corresponds to $s = \frac{1+r-\tau}{1+\gamma} = 1$ and $a = \frac{g}{1+\gamma} = 0$, such that the map w defined in (7) ceases to be contractive and becomes the identity map $w(x) = x$. Of course, by losing the contractivity property, the fixed point of operator T^* in (11) is no longer unique and becomes dependent of the initial density u_0. Specifically, the fixed point is the initial density u_0 itself, since:

$$T^* u_0(x) = \frac{1+\gamma}{1+r-\tau} u_0\left[w^{-1}(x)\right] = u_0(x)$$

because $\frac{1+\gamma}{1+r-\tau} = \frac{1}{s} = 1$ and $w^{-1}(x) = x$. In other words, in this peculiar case any density u turns out to be invariant under operator T^*.

4 The Model under Ambiguity

Thus far, the only form of uncertainty in our model is related to the randomness in the financial market's expectations which makes the interest rate and thus the debt ratio random variables. There is however an additional layer of uncertainty that we need to take into account, related to the limited knowledge on parameter values. Indeed, policymakers need to set the fiscal policy instruments to stabilize the public debt by considering the possible values of the growth rate and the interest rate: the interest rate is unpredictable due to the frequent changes in financial market's expectations but also the growth rate cannot be taken for granted since economic production is highly volatile. Therefore, in order to account for such a vague knowledge on the relevant parameters, policymakers need to rely on their subjective assessment to forecast them despite such assessment may or may not be met in reality. In particular, they need to form some synthetic assessment of the interest rate (*i.e.*, the mean) to quantify how it may be affected by the stochasticity in the financial market's expectations.

We now add such an additional layer on uncertainty by introducing ambiguity in our framework. Specifically, policymakers develop N different assessments of the parameters r and γ, setting accordingly the value of the fiscal policy tools τ and g. In our setup this process translates into the existence of N maps:

$$w_i(x) := \frac{1 + r_i - \tau_i}{1 + \gamma_i} x + \frac{g_i}{1 + \gamma_i}, \tag{14}$$

associated with the different assessments developed by the policymakers, such that each map is characterized by a different set of interest rate on borrowing, r_i, growth rate of output, γ_i, tax rate parameter, τ_i, and public spending share of GDP, g_i. As a matter of analytical simplicity, we assume that these maps satisfy the almost non-overlapping property stated in Assumption A.1.

Since the different policymakers' assessments are subjectively formed and thus it is impossible to state which of them may be most likely, for the sake of simplicity we average them to determine the evolution of the density of the debt ratio. Therefore, we take the average and reassemble the actions of the different maps w_i on u_t to produce u_{t+1}, such that our ambiguity-extended model reads as follows:

$$u_{t+1} = T_N^* u_t \tag{15}$$

where:

$$T_N^* u := \frac{1}{N} \sum_{i=1}^{N}{}' \frac{1 + \gamma_i}{1 + r_i - \tau_i} u \circ w_i^{-1}, \tag{16}$$

where, as usual, the prime means that the sum operates only on those terms for which $w_i^{-1} \in [0, 1]$. According to (15) and (16), at each iteration, the density of the debt ratio at time $t + 1$ is obtained by averaging modified copies of the empirical distribution of the debt ratio under the different assessments during the previous period.

We can easily prove that T_N^* maps the space of densities U into itself and it is Lipschitz with Lipschitz constant equal to:

$$C = \frac{1}{N} \sum_{i=1}^{N} \left(\frac{1 + \gamma_i}{1 + r_i - \tau_i} \right)^{\frac{1}{2}}.$$

Because for all $i = 1, \ldots, N$ condition (8) must hold, it follows that C is greater than one and thus T_N^* is not a contraction on the space of densities U, as it does not satisfy condition (5) in

Proposition 3. However, such a feature, rather than determining multiple fixed points for T_N^*, allows the limit of the orbit generated through the iterations $u_{t+1} = T_N^* u_t$ to lay outside the space of densities U. Specifically, again borrowing from the space of cumulative distribution functions associated to each marginal density u_t as in the previous section, we can establish the uniqueness of the fixed point for the orbit of cumulative distribution functions associated with the orbit generated by $u_{t+1} = T_N^* u_t$. This, in turn, implies that such orbit of densities cannot converge to two distinct invariant distributions, even if such limits do not belong to U.

Recall that the cumulative function F of u is defined as $F(x) = \int_0^x u(v)\,\mathrm{dv}$ and let us define the space of cumulative distribution functions as:

$$\mathcal{F} = \{F : [0,1] \to [0,1],\ F(0) = 0,\ F(1) = 1,\ F \text{ is right-continuous},\ F \text{ is increasing}\}.$$

Through steps similar to those in (13) and recalling that $\frac{1+\gamma_i}{1+r_i-\tau_i} = \frac{1}{s_i}$, we can integrate operator T_N^* in (16) and get its equivalent in terms of cumulative distribution functions:

$$\begin{aligned} F_{t+1}(x) &= \int_0^x u_{t+1}(v)\,\mathrm{dv} = \int_0^x T_N^* u_t(v)\,\mathrm{dv} = \frac{1}{N}\sum_{i=1}^{N}{}' \int_0^x \frac{1}{s_i} u_t\left[w_i^{-1}(v)\right]\mathrm{dv} \\ &= \frac{1}{N}\sum_{i=1}^{N}{}' \frac{1}{s_i}\int_{w_i^{-1}(0)}^{w_i^{-1}(x)} u_t(z)\, w_i'(v)\,\mathrm{dz} = \frac{1}{N}\sum_{i=1}^{N}{}' \int_{w_i^{-1}(0)}^{w_i^{-1}(x)} u_t(z)\,\mathrm{dz} \\ &= \frac{1}{N}\left\{i - 1 + F_t\left[w_i^{-1}(x)\right]\right\} \qquad \text{for } x \in [w_i(0), w_i(1)],\ i = 1,\ldots,N \end{aligned}$$

where in the third equality we use the definition of T_N^* in (16), the fifth equality follows from $w_i'(v) \equiv s_i$, and the last equality holds because, under the almost non-overlapping property (Assumption A.1), for all $i = 1,\ldots,N$ it follows that $\int_{w_i^{-1}(0)}^{w_i^{-1}(x)} u_t(z)\,\mathrm{dz} = 1$ if $x \geq w_i(1)$ and $\int_{w_i^{-1}(0)}^{w_i^{-1}(x)} u_t(z)\,\mathrm{dz} = 0$ if $x \leq w_i(0)$. Hence, we can define the operator $T_N^{\#} : \mathcal{F} \to \mathcal{F}$ as:

$$T_N^{\#} F(x) = \frac{1}{N}\left\{i - 1 + F\left[w_i^{-1}(x)\right]\right\} \qquad \text{for } x \in [w_i(0), w_i(1)], \tag{17}$$

whose fixed-point equation reads as:

$$F(x) = \int_0^x \bar{u}(v)\,\mathrm{dv} = T_N^{\#} F(x) = \frac{1}{N}\left\{i - 1 + F\left[w_i^{-1}(x)\right]\right\} \qquad \text{for } x \in [w_i(0), w_i(1)],$$

where $\bar{u}$ is the fixed point of the operator T_N^*. The following proposition shows that the space $\mathcal{F}$ is complete with respect to the standard d_∞ metric defined as:

$$d_\infty(F,G) = \sup_{x\in[0,1]} |F(x) - G(x)|. \qquad \text{for any } F, G \in \mathcal{F}.$$

Proposition 4. *The space $(\mathcal{F}, d_\infty)$ is a complete metric space.*

Proof. It is well known that d_∞ is a metric. To show that $\mathcal{F}$ is complete, let us take a Cauchy sequence F_n in $\mathcal{F}$ and let us show that $F_n \to F$ with $F \in \mathcal{F}$. For any $x \in [0,1]$, let us define the pointwise limit as $F(x) = \lim_{n\to+\infty} F_n(x)$. It is also clear that $d_\infty(F_n, F) \to 0$ whenever $n \to +\infty$. The only thing to be proved is that $F \in \mathcal{F}$. The pointwise convergence implies that F is increasing, $F(0) = 0$, and $F(1) = 1$. Finally, the uniform convergence allows to conclude that F is right-continuous. ■

Proposition 5. *The operator $T_N^{\#} : \mathcal{F} \to \mathcal{F}$ defined in (17) is contractive with respect to the d_∞ metric and thus it has a unique fixed point.*

Proof. Direct computation leads to

$$\begin{aligned} d_\infty\left(T_N^{\#}F, T_N^{\#}G\right) &= \sup_{x\in[0,1]}\left|\frac{1}{N}\left\{i-1+F\left[w_i^{-1}(x)\right]\right\}-\frac{1}{N}\left\{i-1+G\left[w_i^{-1}(x)\right]\right\}\right| \\ &= \frac{1}{N}\sup_{x\in[w_i(0),w_i(1)]}\left|F\left[w_i^{-1}(x)\right]-G\left[w_i^{-1}(x)\right]\right| \\ &= \frac{1}{N}\sup_{y\in[0,1]}\left|F(y)-G(y)\right| \\ &= \frac{1}{N}d_\infty(F,G), \end{aligned}$$

where in the first two equalities index $i \in \{1,\ldots,N\}$ is determined by x as the unique i satisfying $x \in [w_i(0), w_i(1)]$. This establishes the result whenever $N \geq 2$. ■

Proposition 5 guarantees existence and uniqueness of the fixed point F of $T_N^{\#}$ over $\mathcal{F}$; it actually strengthens Corollary 1 for the case of cumulative distribution functions. This result allows us to conclude that the fixed point of operator T_N^* defined in (16) acting over the space U of densities exists and is unique as well. In fact, if two different fixed points of T_N^* existed, there would be two separate fixed points for operator $T_N^{\#}$ as well, thus contradicting Proposition 5. However, when the limit distribution of operator T_N^* does not lie in the space U, the invariant distribution exhibits singularities at some points of $[0,1]$, possibly being a whole singular probability measure with respect to the Lebesgue measure dx, like in the case of the Dirac distribution obtained in section 3. Despite knowing that such a limit distribution exists and is unique, whenever ambiguity over assessments is introduced, its singularity traits (which definitely follow a much more complex pattern when $N \geq 2$ than the Dirac distribution arising when $N = 1$) make it less predictable than if it were itself a density belonging to the space U.[1] Specifically, probabilities concentrated on single points (or on a zero Lebesgue measure subset of $[0,1]$) make the estimation of the probability that in the long run the debt ratio lies in some subinterval of $[0,1]$ more difficult than in the case of a fixed point which is a density laying in the space U. We shall see in the next section that the presence of some ambiguity aversion allows to smooth such a degree of unpredictability out.

5 Ambiguity Attitude

Thus far, we have simply focused on how the presence of ambiguity affects the public debt ratio by affecting the evolution of its density. We now analyze policymakers' reaction to ambiguity and its consequences on the public debt dynamics. Since our framework is purely dynamic abstracting completely from an optimal decision making process, we assume that a simple rule characterizes entirely policymakers' ambiguity attitude. Specifically, we suppose that they adjust the available vague-information embedded in the empirical distribution with a measure of

[1] To overcome any issue related to the existence of a density in the L^2 space and its interpretation along with the difference between the space of L^2 densities and the space of cumulative distributions, we could formulate an extended operator on the space of distributions $D([0,1])$. This space include, in fact, regular L^p densities as well as singular Dirac-type functionals. An IFS-type operator on $D([0,1])$ has been defined in Forte and Vrscay (1998), but its mathematical formalism and theory go beyond the scope of this paper.

their ignorance embedded in the uniform distribution. Formally, we assume that the N different assessments are associated with weights $\frac{\omega_i}{N}$, $i = 1, \ldots, N$, and maps $w_i(x) = \frac{1+r_i-\tau_i}{1+\gamma_i}x + \frac{g_i}{1+\gamma_i}$ satisfying the almost non-overlapping property (Assumption A.1), such that our extended model to account for ambiguity attitude reads as:

$$u_{t+1} = \frac{1}{N}\sum_{i=1}^{N}{}' \left[\omega_i \left(\frac{1+\gamma_i}{1+r_i-\tau_i}\right) u_t \circ w_i^{-1} + (1-\omega_i)\frac{1+\gamma_i}{1+r_i-\tau_i}\right], \tag{18}$$

where $\omega_i \in [0,1]$. Instead of relying on the arithmetic mean assigning the same weights $\frac{1}{N}$ for all i as in the previous section, in (18) at each iteration the density of the debt ratio at time $t+1$ is obtained as a weighted average of the previous period's modified copies of its empirical distribution by means of different weights $\frac{\omega_i}{N}$, each of them determined by $\omega_i \leq 1$, for all $i = 1, \ldots, N$. In the definition of such weights, $\omega_i < 1$ suggests that the policymakers assign only a certain level of reliability to the information provided by the empirical density u_t when assessment i is considered. Such partial reliability of the empirical distribution is adjusted through a term which measures policymakers' ignorance regarding the true parameter values, captured by the second additive term in the square bracket in (18). Whenever $\omega_i < 1$, the positive constant $(1-\omega_i)\frac{1+\gamma_i}{1+r_i-\tau_i}$ is (uniformly) added to each term $\left(\frac{1+\gamma_i}{1+r_i-\tau_i}\right) u_t \circ w_i^{-1}$, the latter being itself diminished by the multiplicative coefficient $\omega_i < 1$. We may therefore interpret ω_i as the "degree of ambiguity tolerance" and its complement to 1, $(1-\omega_i)$, as the "degree of ambiguity aversion". Note that when $\omega_i = 1$ for all $i = 1, \ldots, N$ this model boils down to the one presented in the previous section.

Our above model's specification states that whenever $\omega_i < 1$ the dynamic described in (18) at time $t+1$ produces a distorted copy of u_t for assessment i exhibiting a larger level of uncertainty than that observed at time t through u_t; such an increase in uncertainty is obtained by adding the constant (uniform) probability $(1-\omega_i)\frac{1+\gamma_i}{1+r_i-\tau_i}$ to each value of $u_t(x)$, for all $x \in [0,1]$. The latter constant term adds some measure of ignorance to the distribution in the current period, u_t, determining a next period's density, u_{t+1}, which becomes flatter (*i.e.*, closer to the uniform density $u(x) \equiv 1$) than the distorted copy of u_t that would result without such additive constant. This means that the i-th assessment exhibits an increasing level of uncertainty as time elapses, or, equivalently, that, after each iteration of system (18), the probability of less likely outcomes becomes proportionally larger than that of more likely outcomes in relative terms. Therefore, our setup suggests that the presence of ambiguity aversion increases the level of uncertainty by increasing the weight of unlikely outcomes. The following example may help to interpret this property.

Example 1. *Let $v : [0,1] \to \mathbb{R}_+$ be defined by $v(x) = 2x$; clearly $v(x)$ is a density because $\int_0^1 2x\,\mathrm{dx} = 1$. Let $\omega = \frac{1}{2}$ and consider the transformation $u(x) = \omega v(x) + (1-\omega) = x + \frac{1}{2}$; clearly $u(x)$ is still a density on $[0,1]$ as $\int_0^1 \left(x + \frac{1}{2}\right)\mathrm{dx} = 1$. However, with respect to $v(x)$, $u(x)$ represents a flatter density concentrating larger probabilities on values x closer to 0 and lower probabilities on values x closer to 1 than $v(x)$ does.*

Our extended model can thus be written as a dynamical system by defining the following operator T:

$$Tu := \frac{1}{N}\sum_{i=1}^{N}{}' \left[\omega_i \left(\frac{1+\gamma_i}{1+r_i-\tau_i}\right) u \circ w_i^{-1} + (1-\omega_i)\frac{1+\gamma_i}{1+r_i-\tau_i}\right]. \tag{19}$$

where, again, the prime means that the sum operates only on those terms for which $w_i^{-1} \in [0,1]$. Given that $u_0 \in U$ is the density of x_0, the density u_{t+1} can be obtained by the action of the

operator T on u_t, that is, $u_{t+1} = Tu_t$. This means that operator T is defined according to (4) whose constituents are the maps $w_i(x) = s_i x + a_i$ of the type defined by (1) with

$$s_i = \frac{1 + r_i - \tau_i}{1 + \gamma_i} \qquad \text{and} \qquad a_i = \frac{g_i}{1 + \gamma_i}, \tag{20}$$

together with greyscale maps $\phi_i(y) = \alpha_i y + \beta_i$ of the type defined by (2) with

$$\alpha_i = \frac{\omega_i}{N}\left(\frac{1 + \gamma_i}{1 + r_i - \tau_i}\right) \qquad \text{and} \qquad \beta_i = \frac{1 - \omega_i}{N}\left(\frac{1 + \gamma_i}{1 + r_i - \tau_i}\right) \tag{21}$$

for all $i = 1, \ldots, N$.

We are now ready to establish our main result. It states that, unlike the model based on a simple average of assessments discussed in section 4 in which the limiting distribution may exhibit singularity features that increase its level of unpredictability, the ambiguity aversion characterizing the policymakers' response to vagueness in past information, represented by the terms ω_i, under certain conditions may ensure that the dynamic generated by (19) converges to a unique invariant density characterizing a much smoother tool to estimate probabilities in the long run. The conditions needed broadly require that on average there is enough ambiguity aversion in the response to the vague information associated with the i assessments, for $i = 1, \ldots, N$. Let U be the space of all densities functions as introduced in Definition 2 and note that the parameters' choices in (20) and (21) satisfy property ii) of Proposition 3, so that the following proposition is just an application of the previous Proposition 3.

Proposition 6. *Suppose that Assumption A.1 holds true together with the following conditions:*

i) *parameters r_i, γ_i, τ_i and g_i satisfy condition (8), that is,*

$$0 \leq \frac{1 + r_i - \tau_i}{1 + \gamma_i} < \frac{1 + r_i - \tau_i + g_i}{1 + \gamma_i} \leq 1 \qquad \textit{for } i = 1...N,$$

ii)

$$\frac{1}{N}\sum_{i=1}^{N} \omega_i \left(\frac{1 + \gamma_i}{1 + r_i - \tau_i}\right)^{\frac{1}{2}} < 1.$$

Then the debt-to-GDP ratio dynamics model defined by

$$u_{t+1} = Tu_t = \frac{1}{N}\sum_{i=1}^{N}{}' \left[\omega_i \left(\frac{1 + \gamma_i}{1 + r_i - \tau_i}\right) u_t \circ w_i^{-1} + (1 - \omega_i)\left(\frac{1 + \gamma_i}{1 + r_i - \tau_i}\right)\right]$$

has a unique fixed (steady-state) point $\bar{u} \in U$ that is also a global attractor, namely:

$$u_n \underset{L^2}{\to} \bar{u},$$

for any initial condition $u_0 \in U$. Moreover, $\bar{u}$ is characterized by the following expression:

$$\bar{u} = \frac{1}{N}\sum_{i=1}^{N}{}' \left[\omega_i \left(\frac{1 + \gamma_i}{1 + r_i - \tau_i}\right) \bar{u} \circ w_i^{-1} + (1 - \omega_i)\left(\frac{1 + \gamma_i}{1 + r_i - \tau_i}\right)\right]. \tag{22}$$

Unlike what we have seen in section 4, Proposition 6 shows that the unique fixed point for our extended model is still an element of the space U, that is, a density, as under assumption ii) operator T defined in (19) is a contraction according to Proposition 1 and thus all the results in Proposition 3 directly extend to our model as well. Moreover, equation (22) shows that $\bar{u}$ is a self-similar object as it is the sum of distorted copies of itself. Note that condition ii) requires ambiguity tolerance coefficients ω_i to be sufficiently small on average. In other words, a sufficient level of ambiguity aversion—represented by the complement coefficients $(1-\omega_i)$—is necessary in order to smooth out singularities upon the limiting density that may appear in the model without ambiguity attitudes of section 4. Paradoxically, the unpredictability of a stochastic dynamic like that defined by (15) is being smoothed out by adding more uncertainty to the system. Of course there is a trade-off: on the one hand, the additional uncertainty originated by the constant terms $(1-\omega_i)\frac{1+\gamma_i}{1+r_i-\tau_i}$ in the operator T defined by (19) leads to a limiting density that is flatter (closer to the uniform density), and thus less informative, than the fixed points of operator T_N^* defined in (16); on the other hand, whenever assumption ii) in Proposition 6 is met—that is, in presence of a sufficient level of ambiguity aversion—the limiting density becomes perfectly predictable. Hence, there is a price to pay for predictability: a flatter (more uniform), less informative limiting density that, however, can be completely foregone.

The following corollary helps us to appreciate how adding more uncertainty to the system after each iteration according to operator T in (19) when the contractivity assumption ii) of Proposition 6 is satisfied affects the limiting density by showing that, when the assessments considered by policymakers are "symmetric" (specifically, the maps w_i are wavelets), the fixed point of operator T in (19) is the uniform density itself regardless of the initial density u_0, that is, the system always converges to the most uninformative distribution.

Corollary 3. *Under conditions i) and ii) of Proposition 6 assume further that the maps w_i are wavelets, that is, suppose that*

$$s_i = \frac{1+r_i-\tau_i}{1+\gamma_i} = \frac{1}{N} \qquad \textit{and} \qquad a_i = \frac{g_i}{1+\gamma_i} = \frac{i-1}{N} \qquad \textit{for } i = 1,\ldots,N. \tag{23}$$

Then operator T defined in (19) has always the uniform density $\bar{u}(x) \equiv 1$ as its unique fixed point for any initial density $u_0(x)$.

Proof. As under condition ii) of Proposition 6 operator T in (19) is a contraction, to guarantee existence and uniqueness of its fixed point it is enough to find a density $\bar{u}$ satisfying equation (22):

$$\begin{aligned} \bar{u} = T\bar{u} &= \frac{1}{N}\sum_{i=1}^{N}{}' \left[\omega_i \left(\frac{1+\gamma_i}{1+r_i-\tau_i}\right)\bar{u}\circ w_i^{-1} + (1-\omega_i)\left(\frac{1+\gamma_i}{1+r_i-\tau_i}\right)\right] \\ &= \frac{1}{N}\sum_{i=1}^{N}{}' \left[\omega_i N\bar{u}\circ w_i^{-1} + (1-\omega_i)N\right] = \sum_{i=1}^{N}{}' \left[\omega_i \bar{u}\circ w_i^{-1} + (1-\omega_i)\right] \end{aligned} \tag{24}$$

where in the third equality we used the first condition in (23). If we replace $\bar{u}(x) \equiv 1$ into the last term of (24) we have $\bar{u}\circ w_i^{-1} \equiv 1$ for all $i = 1,\ldots,N$, so that

$$\bar{u}(x) = (T\bar{u})(x) = \sum_{i=1}^{N}{}' \left[\omega_i + (1-\omega_i)\right] = \sum_{i=1}^{N}{}' 1 = 1 \equiv \bar{u}(x),$$

where the fourth equality holds because the prime in the sum implies that we are actually taking the union of the constant 1 over the partition of $[0,1]$ formed by the subintervals of size $\frac{1}{N}$ that, according to condition (23), are the sets $w_i([0,1])$ for $i = 1, \ldots, N$; specifically, $w_1([0,1]) = \left[0, \frac{1}{N}\right]$, $w_2([0,1]) = \left[\frac{1}{N}, \frac{2}{N}\right], \ldots, w_N([0,1]) = \left[\frac{N-1}{N}, 1\right]$. ■

Note that calculations similar to those in the last part of the proof of Corollary 3 hold also for operator T_N^* defined (16) for the model discussed in section 4, so that, whenever the the maps w_i are wavelets, the unique fixed point for T_N^* *does* belong to the space U of densities, being it always the uniform density regardless of the initial density u_0. This fact will be illustrated in the next section.

6 Numerical Simulations

Thanks to the "piecewise" routine embedded in Maple we built a simple algorithm that directly iterates the definition of operator T in (19) by transforming any density u_t into its next step density u_{t+1}.[2] There is no need to keep track of all intervals in each pre-fractal (*i.e.*, the images of the maps w_i after each iteration) as the piecewise function routine in Maple does it automatically. This feature together with the symbolic computation of integrals in Maple allows us to start from any initial density u_0 on $[0,1]$ which is integrable in closed-form and follow its transformation after each iteration to appreciate how exactly operator T shrinks 'horizontally' and modifies 'vertically' the marginal density u_t. While the algorithm works also under the strong no overlap condition—introducing 'holes' among the image sets $w_i([0,1])$ after each iteration so to have a Cantor-like set as support for the limiting distribution—we will consider only examples satisfying the almost non-overlapping property (Assumption A.1). We follow the order in which we introduced the three operators T^* according to (11), T_N^* according to (16) and T according to (19) in sections 3, 4 and 5 respectively. We consider at most three different assessments $i = 1, 2, 3$, and in all assessments we fix the exogenous growth rate at the constant level $\gamma = 0.02$ while the exogenous international interest rate is assumed to take the following three different values $r_1 = 0.02$, $r_2 = 0.05$, $r_3 = 0.08$.

Our first exercise aims at illustrating the behavior of the algorithm in the benchmark model considered in section 3, that is, we apply it to operator T^* defined in (11). Assuming $\gamma = 0.02$ and $r = 0.02$, we set $\tau = 0.51$ and $g = 0.255$, so that the (unique) map $w(x) = sx + a$ has parameters $s = \frac{1+r-\tau}{1+\gamma} = \frac{1}{2}$ and $a = \frac{g}{1+\gamma} = \frac{1}{4}$ respectively, while its unique fixed point is $\bar{x} = \frac{g}{\gamma - r + \tau} = \frac{1}{2}$; the (unique) greyscale map $\phi(y) = \alpha y + \beta$ has parameters $\alpha = \frac{1+\gamma}{1+r-\tau} = \frac{1}{s} = 2$ and $\beta = 0$. In this case operator T^* does not satisfy Assumption A.1 because the image set of the map $w(x)$ is a proper subset of $[0,1]$ and is not contractive; however, it has the unique fixed point represented by the Dirac distribution $\delta_{\frac{1}{2}}(x)$ concentrating all the probability on the fixed point $\bar{x} = \frac{1}{2}$, regardless of the initial density u_0. Figure 1 plots the first 7 iterations of operator T^* starting from the bimodal initial density $u_0(x) = 12\left(x - \frac{1}{2}\right)^2$ as obtained by running our Maple algorithm: after each iteration operator T^* clearly shrinks the support of the marginal density u_t while augmenting its height, letting the dynamic converge to $\delta_{\frac{1}{2}}(x)$ as $t \to \infty$. Figure 2 plots the evolution of the corresponding cumulative distribution functions F_t associated to the densities u_t in Figure 1.

[2]The detailed code is available upon request.

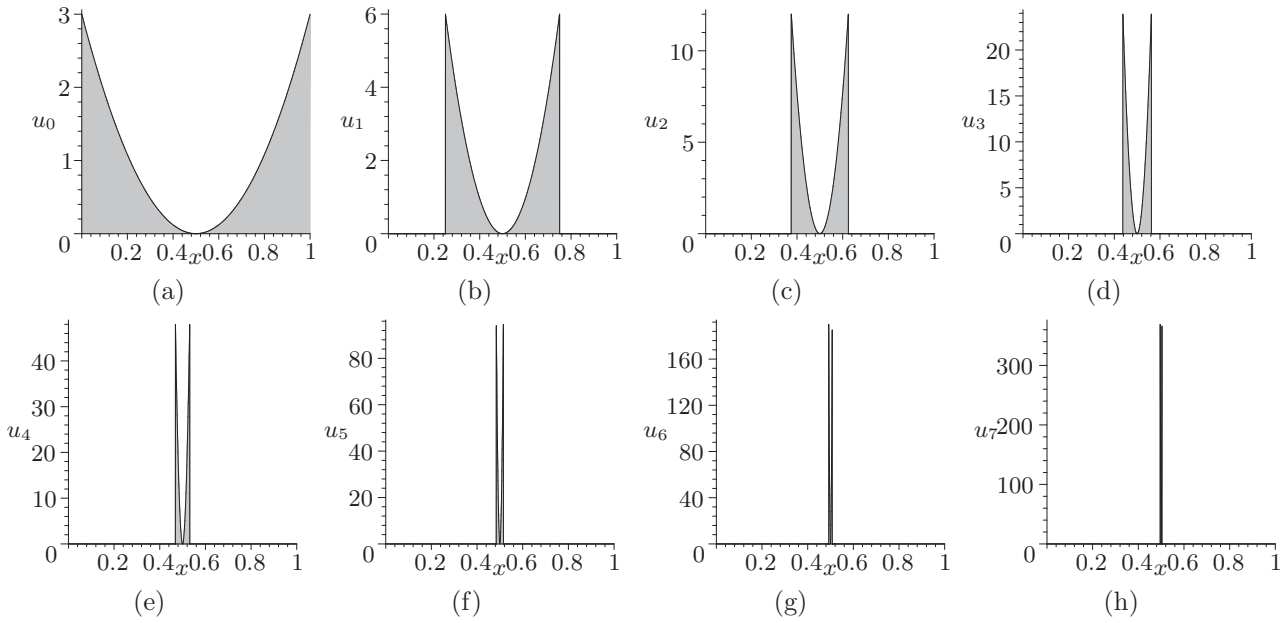

FIGURE 1: First 7 iterations of operator T^* defined in (11) for the only map $w(x) = \frac{1}{2}x + \frac{1}{4}$ together with the only greyscale map $\phi(y) = 2y$ starting from $u_0(x) = 12\left(x - \frac{1}{2}\right)^2$.

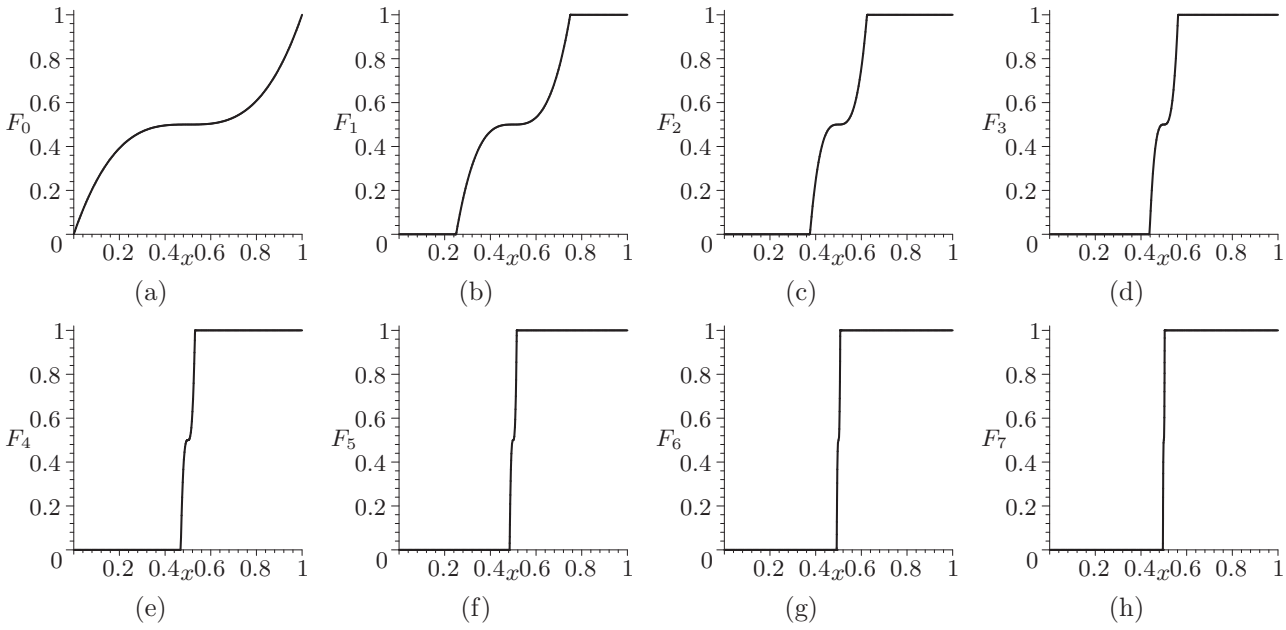

FIGURE 2: cumulative distribution functions associated to the densities u_t in Figure 1.

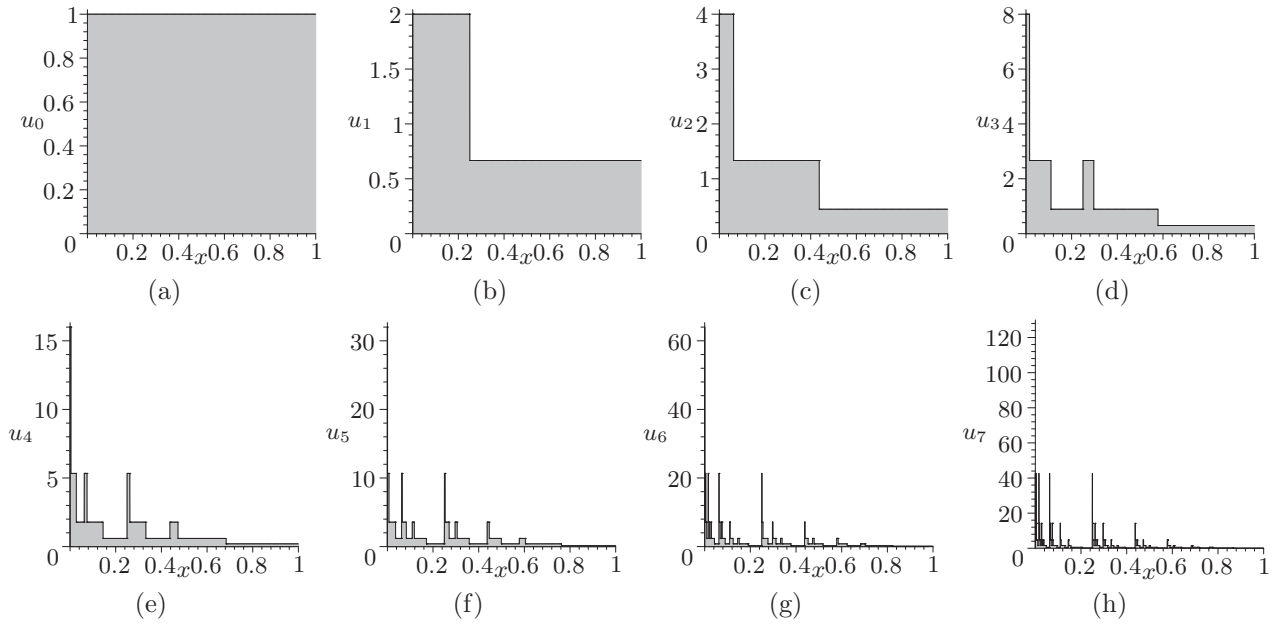

FIGURE 3: First 7 iterations of operator T_2^* defined in (16) for the maps $w_1(x) = \frac{1}{4}x$ and $w_2(x) = \frac{3}{4}x + \frac{1}{4}$ together with greyscale maps $\phi_1(y) = 2y$ and $\phi_2(y) = \frac{2}{3}y$ starting from $u_0(x) \equiv 1$.

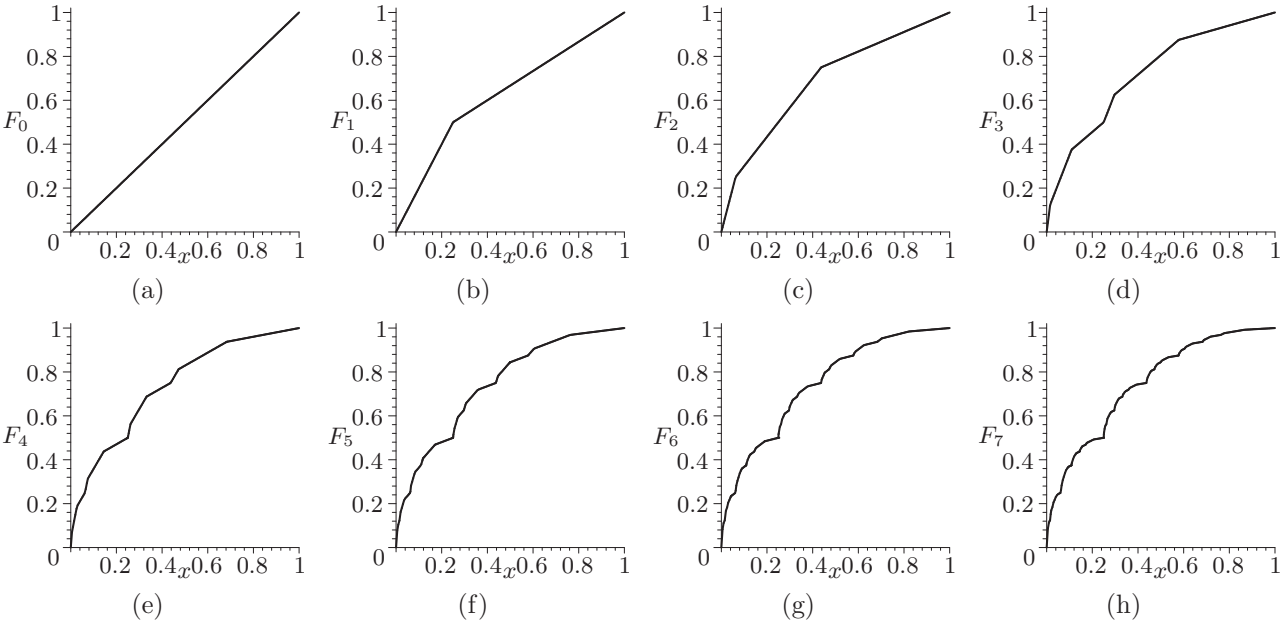

FIGURE 4: cumulative distribution functions associated to the densities u_t in Figure 3.

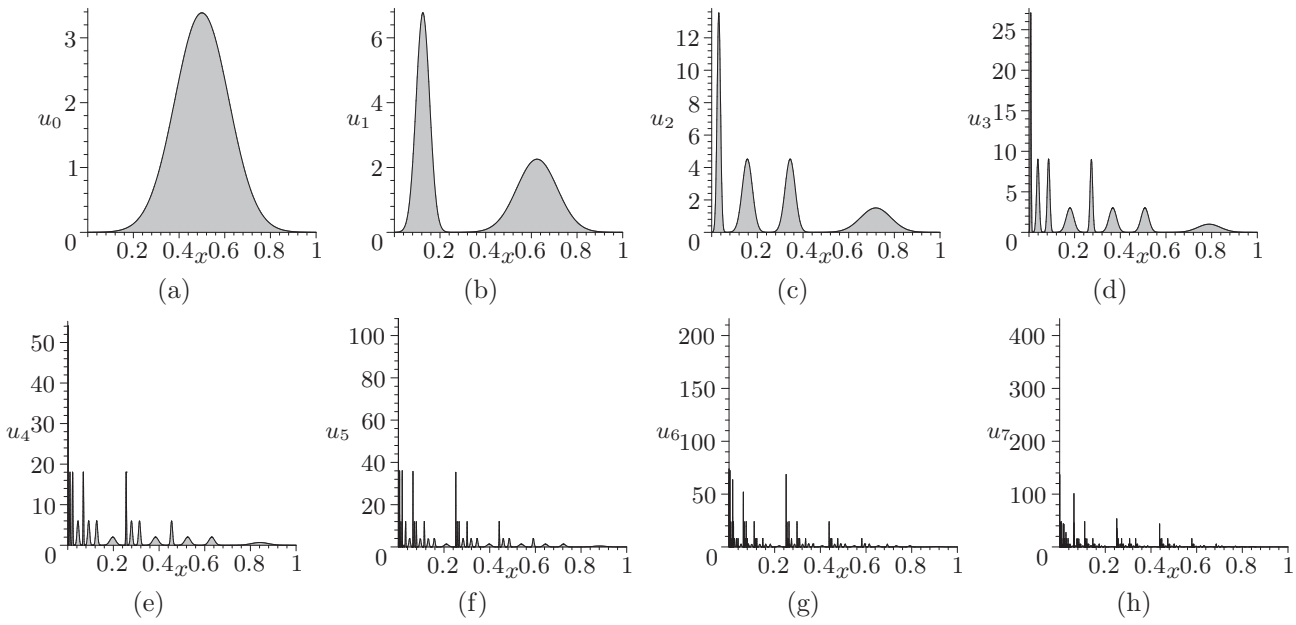

FIGURE 5: First 7 iterations of operator T_2^* defined in (16) for the maps $w_1(x) = \frac{1}{4}x$ and $w_2(x) = \frac{3}{4}x + \frac{1}{4}$ together with greyscale maps $\phi_1(y) = 2y$ and $\phi_2(y) = \frac{2}{3}y$ starting from $u_0(x) = 3.3852e^{-(6x-3)^2}$.

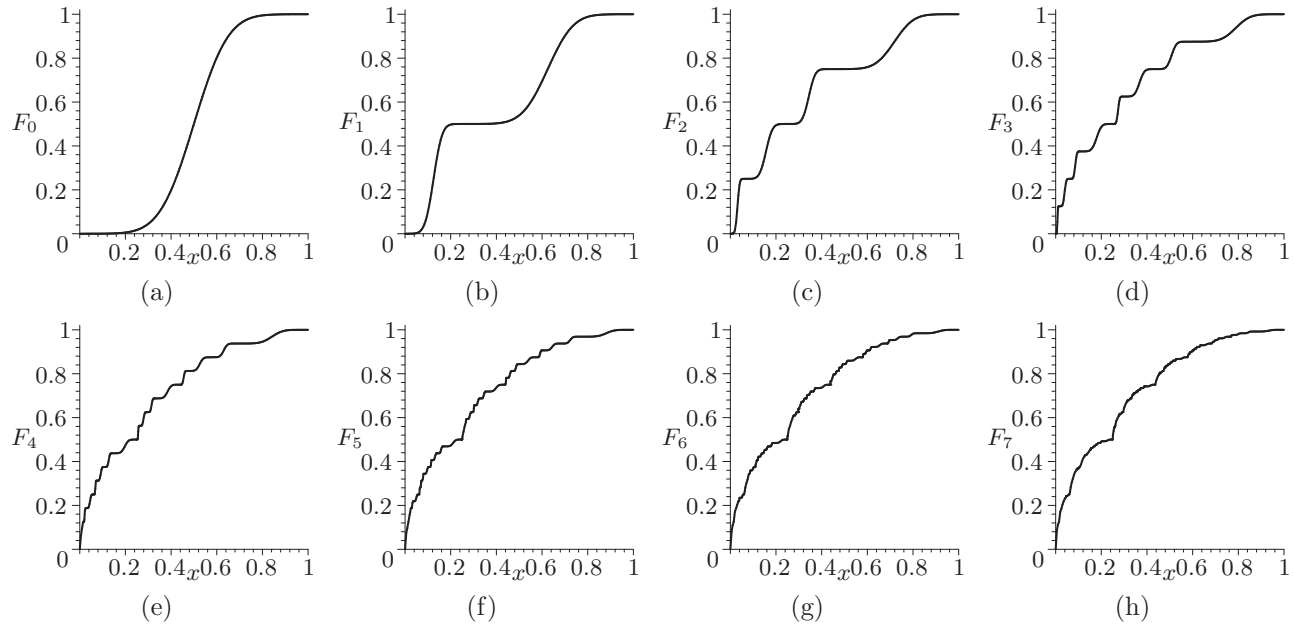

FIGURE 6: cumulative distribution functions associated to the densities u_t in Figure 5.

Next, we apply our algorithm to an example with $N = 2$ assessments of the type discussed in section 4 for which we consider the following pair of parametrizations.: $\gamma = 0.02$, $r_1 = 0.02$, $\tau_1 = 0.765$, $g_1 = 0$, and $\gamma = 0.02$, $r_2 = 0.05$, $\tau_2 = 0.285$, $g_2 = 0.255$, so that the maps $w_i(x) = s_i x + a_i$ have parameters $s_1 = \frac{1+r_1-\tau_1}{1+\gamma} = \frac{1}{4}$, $a_1 = \frac{g_1}{1+\gamma} = 0$ and $s_2 = \frac{1+r_2-\tau_2}{1+\gamma} = \frac{3}{4}$, $a_2 = \frac{g_2}{1+\gamma} = \frac{1}{4}$ respectively, while the greyscale maps $\phi_i(y) = \alpha_i y + \beta_i$ have parameters $\alpha_1 = \frac{1+\gamma}{2(1+r_1-\tau_1)} = \frac{1}{2s_1} = 2$ and $\alpha_2 = \frac{1+\gamma}{2(1+r_2-\tau_2)} = \frac{1}{2s_2} = \frac{2}{3}$ with $\beta_1 = \beta_2 = 0$. In this case

the operator T_2^* defined in (16) satisfies Assumption A.1—so that the union of the images of the maps $w_1([0,1]) \cup w_2([0,1])$ is the whole interval $[0,1]$ while such images almost do no overlap—but again it is not a contraction. Figure 3 plots the first 7 iterations of operator T_2^* as obtained by running our Maple algorithm starting from the uniform initial density $u_0(x) \equiv 1$, while Figure 4 reports the corresponding cumulative distribution functions F_t associated to them. Figure 5 shows the first 7 iterations of the same operator T_2^* but now starting from the bell-shaped initial density $u_0(x) = 3.3852e^{-(6x-3)^2}$, while Figure 6 reports the corresponding cumulative distribution functions F_t. Clearly, Figures 3 and 5—as well as Figures 4 and 6 for the cumulative distribution functions—report different graphs for the first iterations because the algorithm starts from different initial densities u_0; however, already after the 5^{th} iteration they start looking similar in qualitative terms. Although the spike of the first modified copy of the initial density u_0—that closest to 0 in Figure 5(b)—in Figure 5 keeps being more than three times taller than the analogous one in Figure 3 after each iteration, Proposition 5 assures that both sequences of marginal densities u_t must converge to the same fixed point as $t \to \infty$, which may possibly be a singular measure.

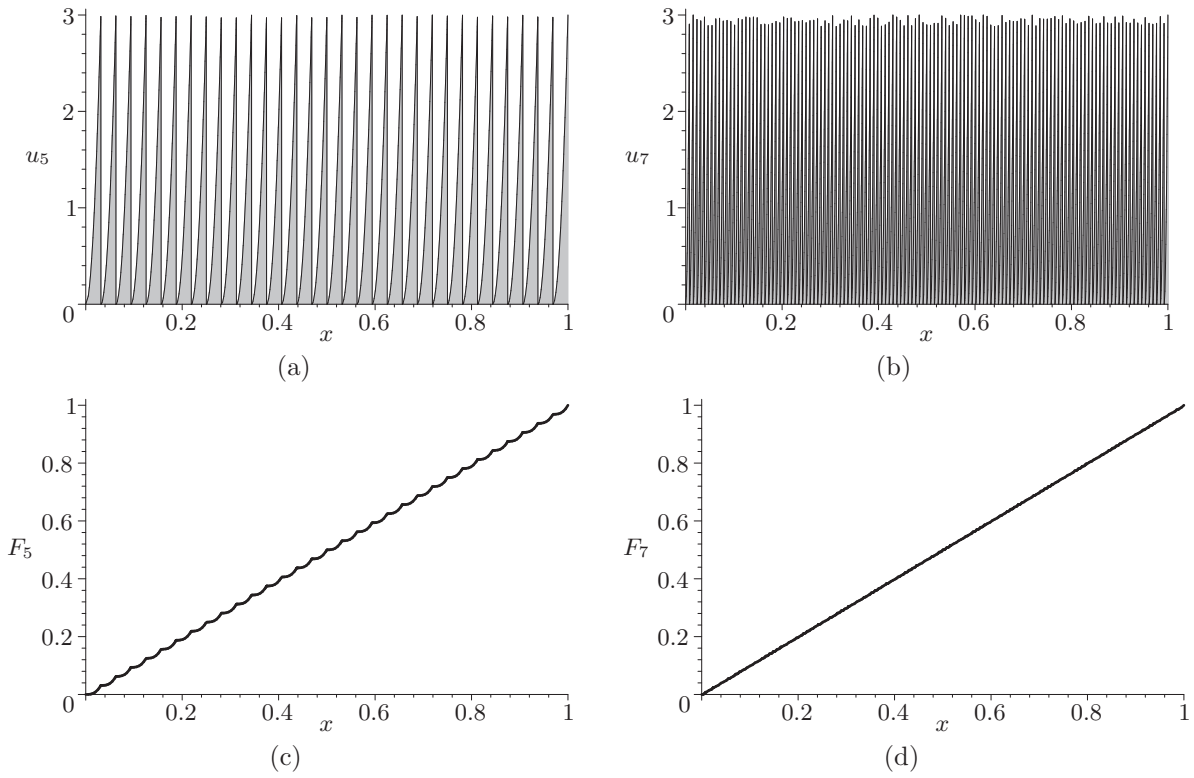

FIGURE 7: a) 5^{th} and b) 7^{th} iteration of operator T_2^* defined in (16) for the wavelets maps $w_1(x) = \frac{1}{2}x$ and $w_2(x) = \frac{1}{2}x + \frac{1}{2}$ together with greyscale maps $\phi_1(y) = \phi_2(y) = y$ starting from $u_0(x) = 3x^2$, c) and d) cumulative distribution functions associated to the densities u_5 and u_7.

As observed at the end of section 5 after Corollary 3, if the maps w_i are *wavelets* the uniform density is the unique fixed point for the operator T_N^* defined in (16). Of course, if the initial density is the uniform density itself our algorithm just replicates the same uniform density after each iteration; hence, it is more interesting to check the evolution of the transition densities when the initial density u_0 is different than $u_0(x) \equiv 1$. Suppose that $N = 2$ with the following pair of parametrizations.: $\gamma = 0.02$, $r_1 = 0.02$, $\tau_1 = 0.51$ $g_1 = 0$, and $\gamma = 0.02$, $r_2 = 0.05$, $\tau_2 = 0.54$, $g_2 = 0.51$, so that the maps $w_i(x) = s_i x + a_i$ turn out to be wavelets defined by

$s_1 = s_2 = \frac{1+r_1-\tau_1}{1+\gamma} = \frac{1+r_2-\tau_2}{1+\gamma} = \frac{1}{2}$, $a_1 = \frac{g_1}{1+\gamma} = 0$, $a_2 = \frac{g_2}{1+\gamma} = \frac{1}{2}$ respectively, while the greyscale maps $\phi_i(y) = \alpha_i y + \beta_i$ have parameters $\alpha_1 = \alpha_2 = \frac{1}{2s_1} = \frac{1}{2s_2} = 1$ with $\beta_1 = \beta_2 = 0$. Figures 7(a) and 7(b) show the 5^{th} and the 7^{th} iterations of operator T_2^* respectively as obtained by running our Maple algorithm starting from the increasing initial density $u_0(x) = 3x^2$, while, as usual, Figures 7(c) and 7(d) reports the associated cumulative distribution function. In Figure 7(a) the $2^5 = 32$ shrunk copies of the initial increasing density $u_0(x) = 3x^2$ (the half parabolas) are still apparent, while in Figure 7(b) there are $2^7 = 128$ (more squeezed) copies so that they become hard to discern. Clearly, because $\alpha_1 = \alpha_2 = 1$ and $\beta_1 = \beta_2 = 0$, the spikes of all half parabolas remain at level $u_0(1) = 3 > 1$ after all iterations, thus misleading into the wrong conclusion that the limiting fixed point should be something different than the uniform density. However, Proposition 5, establishing uniqueness of the fixed point, together with our knowledge of $u_0(x) \equiv 1$ being a fixed point, guarantee that also the marginal densities in Figure 7 must converge to the uniform density as $t \to \infty$. This implies that after a sufficiently large number of iterations operator T_2^* tends to concentrate all probability into the square $[0,1]^2$, that is, on the lower third portion of all the half parabolas visible in Figure 7(a).

The next example considers $N = 3$ assessments of the type discussed in section 4 for which we consider the following set of parametrizations.: $\gamma = 0.02$, $r_1 = 0.02$, $\tau_1 = 0.8925$ $g_1 = 0$, $\gamma = 0.02$, $r_2 = 0.05$, $\tau_2 = 0.6675$, $g_2 = 0.1275$, and $\gamma = 0.02$, $r_3 = 0.08$, $\tau_3 = 0.57$, $g_3 = 0.51$ so that the maps $w_i(x) = s_i x + a_i$ have parameters $s_1 = \frac{1+r_1-\tau_1}{1+\gamma} = \frac{1}{8}$, $a_1 = \frac{g_1}{1+\gamma} = 0$, $s_2 = \frac{1+r_2-\tau_2}{1+\gamma} = \frac{3}{8}$, $a_2 = \frac{g_2}{1+\gamma} = \frac{1}{8}$ and $s_3 = \frac{1+r_3-\tau_3}{1+\gamma} = \frac{1}{2}$, $a_3 = \frac{g_3}{1+\gamma} = \frac{1}{2}$ respectively, while the greyscale maps $\phi_i(y) = \alpha_i y + \beta_i$ have parameters $\alpha_1 = \frac{1}{3s_1} = \frac{8}{3}$, $\alpha_2 = \frac{1}{3s_2} = \frac{8}{9}$ and $\alpha_3 = \frac{1}{2s_3} = \frac{2}{3}$ with $\beta_1 = \beta_2 = \beta_3 = 0$. Again the operator T_3^* defined in (16) satisfies Assumption A.1 and it is not a contraction; nonetheless, existence and uniqueness of its fixed point are ensured by Proposition 5. Figure 8(a) shows the 5^{th} iteration of operator T_3^* as obtained by running our Maple algorithm starting from the uniform initial density $u_0(x) \equiv 1$, while Figure 8(b) reports the corresponding cumulative distribution function. With $N = 3$ maps the algorithm quickly fills the whole plot after just few iterations, fact that slows it considerably, this is why with three maps we stop it at most after 5 iterations.

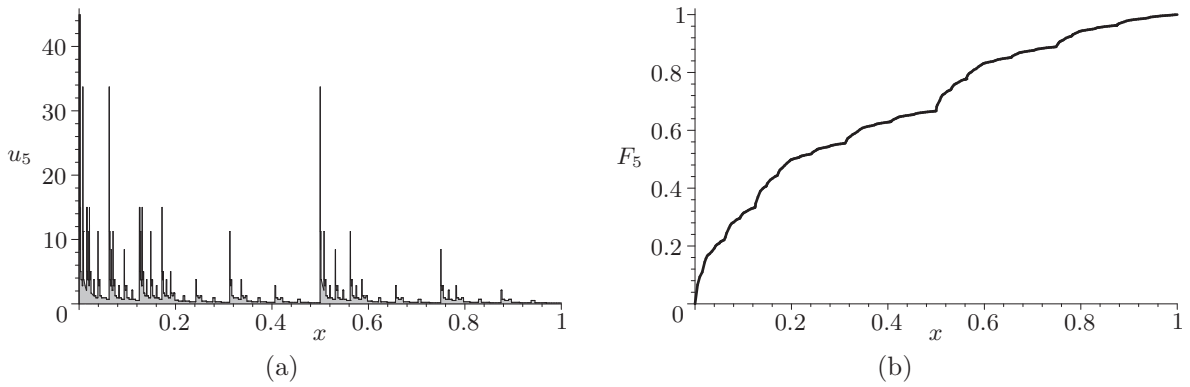

FIGURE 8: a) 5^{th} iteration of operator T_3^* defined in (16) for the maps $w_1(x) = \frac{1}{8}x$, $w_2(x) = \frac{3}{8}x + \frac{1}{8}$ and $w_3(x) = \frac{1}{2}x + \frac{1}{2}$ together with greyscale maps $\phi_1(y) = \frac{8}{3}y$, $\phi_2(y) = \frac{8}{9}y$ and $\phi_3(y) = \frac{2}{3}y$ starting from $u_0(x) \equiv 1$, b) its associated cumulative distribution function.

We now focus on the role played by ambiguity attitudes as introduced in section 5 to define operator T according to (19). We apply our algorithm to the same example with $N = 2$ assessments considered in Figures 3–6, that is, for $\gamma = 0.02$, $r_1 = 0.02$, $\tau_1 = 0.765$, $g_1 = 0$, and

$\gamma = 0.02$, $r_2 = 0.05$, $\tau_2 = 0.285$, $g_2 = 0.255$, so that again $s_1 = \frac{1}{4}$, $a_1 = 0$ and $s_2 = \frac{3}{4}$, $a_2 = \frac{1}{4}$. Now the parameters of the greyscale maps $\phi_i(y) = \alpha_i y + \beta_i$ depend on the degree of ambiguity tolerance ω_i and its complement to 1, $(1 - \omega_i)$: in this first approximation we assume that all ambiguity aversion is associated to the first assessment by setting $\omega_1 = \frac{1}{5}$, while no ambiguity aversion is associated to the second assessment, so that $\omega_2 = 1$. Hence, $\alpha_1 = \frac{\omega_1}{2}\left(\frac{1+\gamma}{1+r_1-\tau_1}\right) = \frac{\omega_1}{2s_1} = \frac{2}{5}$ and $\beta_1 = \frac{1-\omega_1}{2}\left(\frac{1+\gamma}{1+r_1-\tau_1}\right) = \frac{1-\omega_1}{2s_1} = \frac{8}{5}$, while $\alpha_2 = \frac{\omega_2}{2}\left(\frac{1+\gamma}{1+r_2-\tau_2}\right) = \frac{\omega_2}{2s_2} = \frac{2}{3}$ and $\beta_2 = \frac{1-\omega_2}{2}\left(\frac{1+\gamma}{1+r_2-\tau_2}\right) = \frac{1-\omega_2}{2s_2} = 0$. With such a parameterization operator T defined in (19) satisfies Assumption A.1 and it is a contraction, as $\frac{1}{2}\sum_{i=1}^{2}\omega_i\left(\frac{1+\gamma_i}{1+r_i-\tau_i}\right)^{\frac{1}{2}} = \frac{1}{2}\sum_{i=1}^{2}\omega_i s_i^{-\frac{1}{2}} = 0.78 < 1$, so that, according to Proposition 6, its fixed point not only is unique, but is itself a density in the space U starting form any initial density u_0. Figure 9 plots the first 7 iterations of operator T as obtained by running our Maple algorithm starting from the uniform initial density $u_0(x) \equiv 1$, while Figure 10 reports the corresponding cumulative distribution functions F_t. Figure 11 shows the first 7 iterations of the same operator T but now starting from the bell-shaped initial density $u_0(x) = 3.3852e^{-(6x-3)^2}$, while Figure 12 reports the corresponding cumulative distribution functions F_t. It is clear from all four figures that now operator T converges to the same invariant density exhibiting a somewhat decreasing pattern reported in both Figures 9(h) and 11(h).

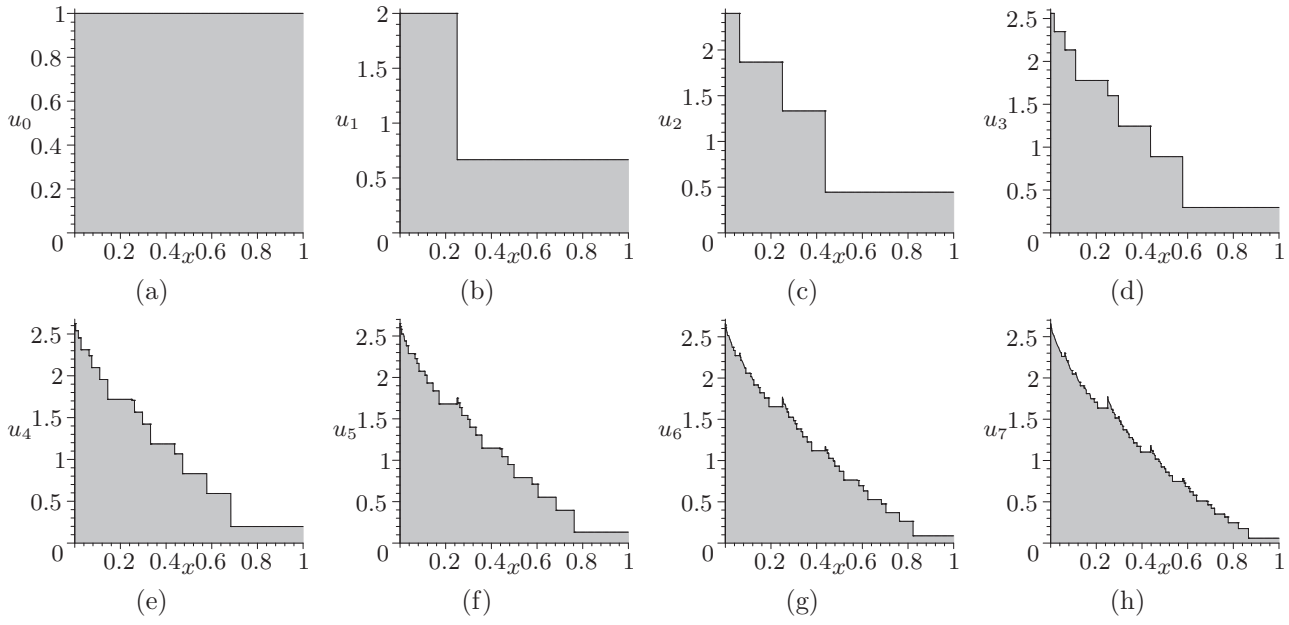

FIGURE 9: First 7 iterations of operator T defined in (19) for the maps $w_1(x) = \frac{1}{4}x$ and $w_2(x) = \frac{3}{4}x + \frac{1}{4}$ together with greyscale maps $\phi_1(y) = \frac{2}{5}y + \frac{8}{5}$ and $\phi_2(y) = \frac{2}{3}y$ starting from $u_0(x) \equiv 1$.

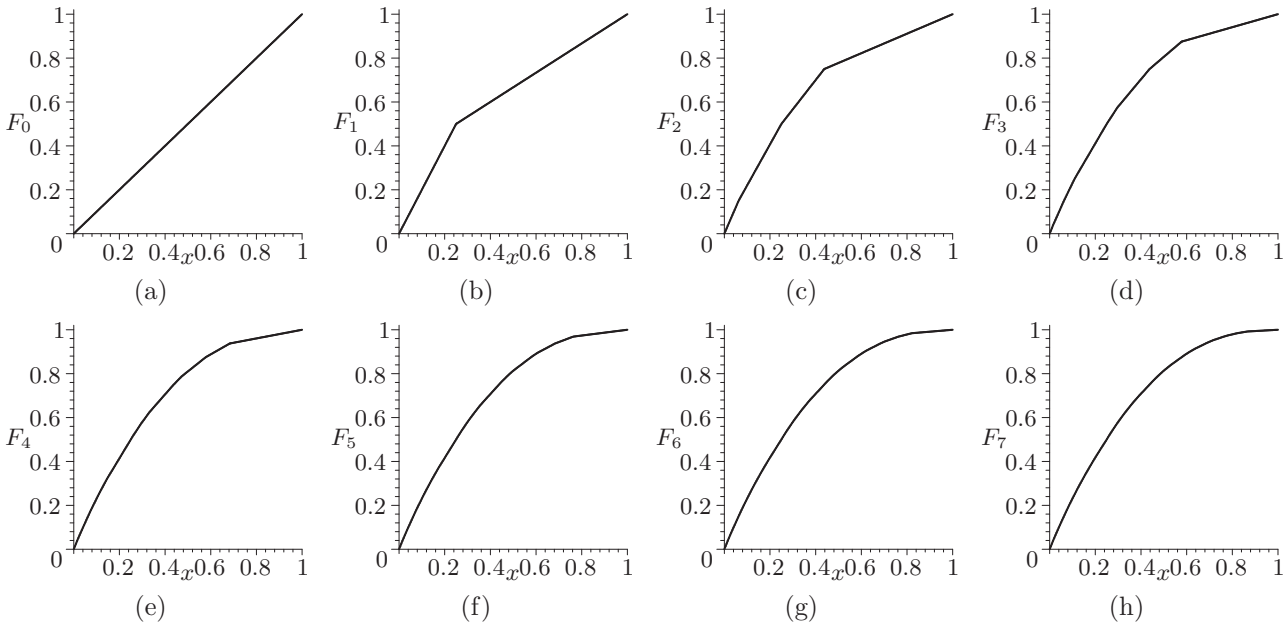

FIGURE 10: cumulative distribution functions associated to the densities u_t in Figure 9.

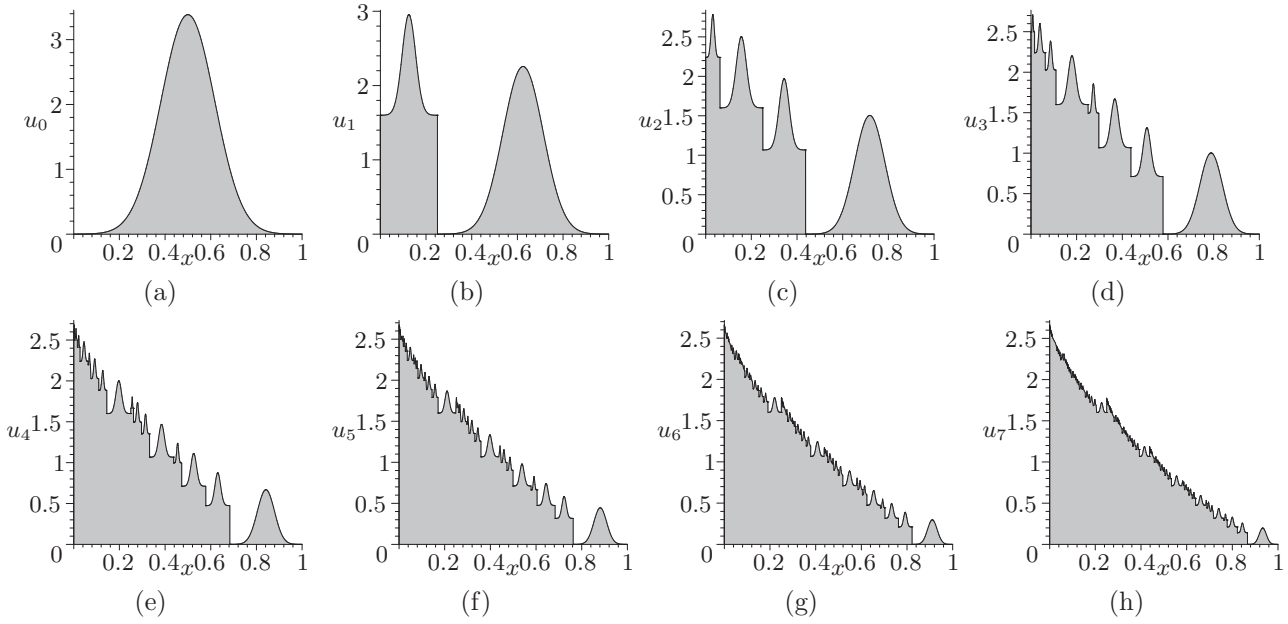

FIGURE 11: First 7 iterations of operator T defined in (19) for the maps $w_1(x) = \frac{1}{4}x$ and $w_2(x) = \frac{3}{4}x + \frac{1}{4}$ together with greyscale maps $\phi_1(y) = \frac{2}{5}y + \frac{8}{5}$ and $\phi_2(y) = \frac{2}{3}y$ starting from $u_0(x) = 3.3852e^{-(6x-3)^2}$.

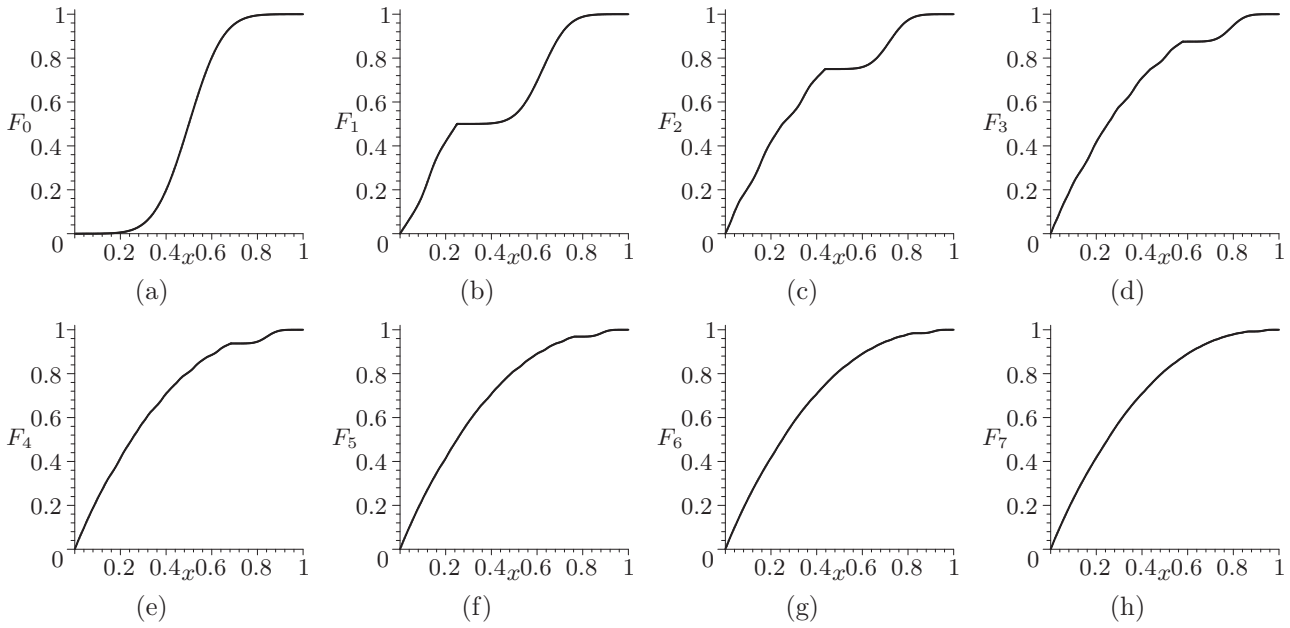

FIGURE 12: cumulative distribution functions associated to the densities u_t in Figure 11.

We now proceed with the same parameters' values for the maps w_i used in the last example described in Figures 9–12 but assume the same ambiguity aversion for both assessments: $\omega_1 = \omega_2 = \frac{1}{2}$. In this case the greyscale maps have parameters $\alpha_1 = \frac{\omega_1}{2s_1} = 1$ and $\beta_1 = \frac{1-\omega_1}{2s_1} = 1$, while $\alpha_2 = \frac{\omega_2}{2s_2} = \frac{1}{3}$ and $\beta_2 = \frac{1-\omega_2}{2s_2} = \frac{1}{3}$. With such a parameterization operator T defined in (19) satisfies Assumption A.1 and is still a contraction, as $\frac{1}{2}\sum_{i=1}^{2} \omega_i s_i^{-\frac{1}{2}} = 0.79 < 1$, so that its fixed point exists, is unique, and is a density in the space U starting form any initial density u_0. Figure 13(a) reports the 7^{th} iteration of operator T as obtained by running our Maple algorithm starting from the uniform initial density $u_0(x) \equiv 1$, which is an approximation of the unique fixed point of operator T, while Figure 13(b) reports the associated cumulative distribution function. Clearly, even if density u_7 in Figure 13(a) still resembles a somewhat decreasing pattern, due to the ambiguity aversion more spread across the two assessments it exhibits a flatter graph than that in Figures 9(h) and 11(h); such a feature emphasizes the role of ambiguity aversion in letting the limit invariant distribution be closer to the uniform density.

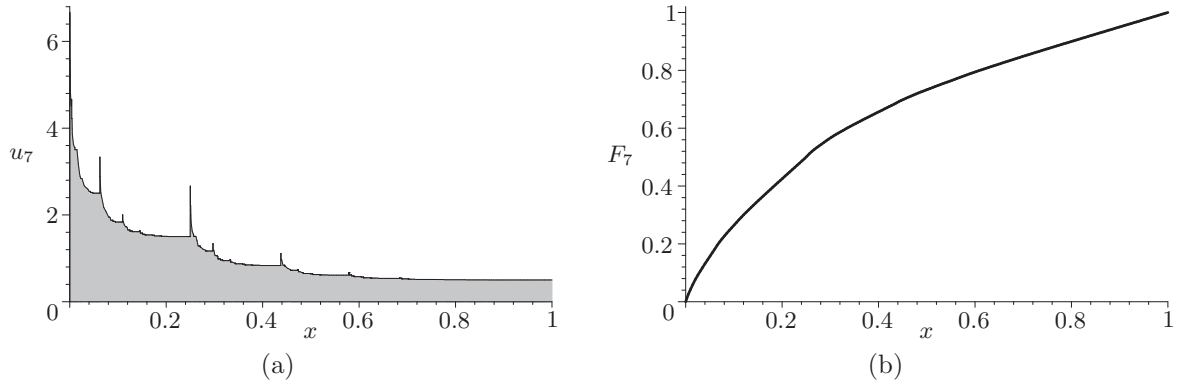

FIGURE 13: a) 7^{th} iteration of operator T defined in (19) for the maps $w_1(x) = \frac{1}{4}x$ and $w_2(x) = \frac{3}{4}x + \frac{1}{4}$ together with greyscale maps $\phi_1(y) = y + 1$ and $\phi_2(y) = \frac{1}{3}y + \frac{1}{3}$ starting from $u_0(x) \equiv 1$, b) its associated cumulative distribution function.

To illustrate Corollary 3 assume that the $N = 2$ maps w_i are wavelets; such a configuration, for example, is obtained with $\gamma = 0.02$, $r_1 = 0.02$, $\tau_1 = 0.51$, $g_1 = 0$, and $\gamma = 0.02$, $r_2 = 0.05$, $\tau_2 = 0.54$, $g_2 = 0.51$, so that $s_1 = s_2 = \frac{1}{2}$, $a_1 = 0$ and $a_2 = \frac{1}{2}$. If the ambiguity aversion parameters are $\omega_1 = \frac{2}{5}$ and $\omega_2 = \frac{4}{5}$ the greyscale maps ϕ_i have parameters $\alpha_1 = \frac{\omega_1}{2s_1} = \frac{2}{5}$ and $\beta_1 = \frac{1-\omega_1}{2s_1} = \frac{3}{5}$, while $\alpha_2 = \frac{\omega_2}{2s_2} = \frac{4}{5}$ and $\beta_2 = \frac{1-\omega_2}{2s_2} = \frac{1}{5}$. Operator T defined in (19) still satisfies Assumption A.1 and it is a contraction, as $\frac{1}{2}\sum_{i=1}^{2}\omega_i s_i^{-\frac{1}{2}} = 0.85 < 1$, so that, according to Corollary 3, must have the uniform density as the unique limit distribution starting form any initial density u_0. Figure 14(a) reports the 7^{th} iteration of operator T as obtained by running our Maple algorithm starting from the bimodal initial density $u_0(x) = 12\left(x - \frac{1}{2}\right)^2$, which provides an approximation of the unique fixed point of operator T, while Figure 14(b) reports the associated cumulative distribution function. Figure 14(a) shows that subsequent iterations of operator T tend to smooth out the spikes of the initial bimodal density, which are maintained in all finite marginal densities u_t, and let them disappear in the limit to converge to the unique fixed point $\bar{u}(x) \equiv 1$.

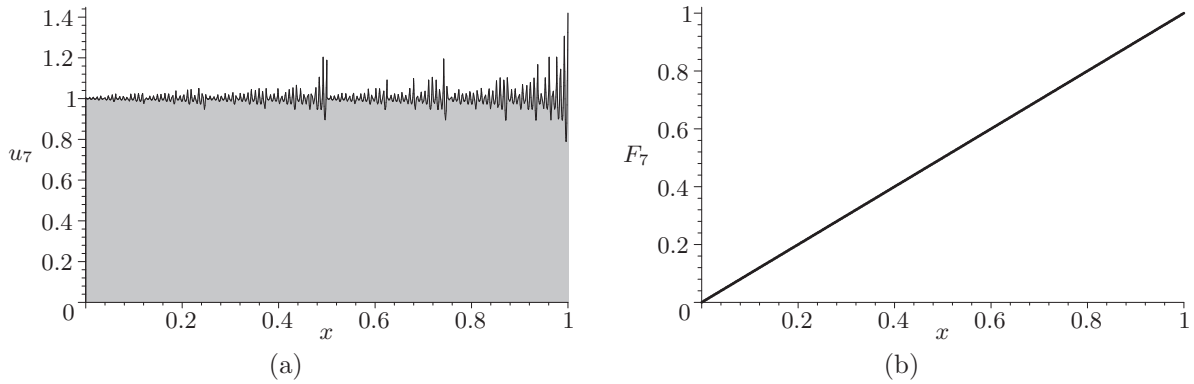

FIGURE 14: a) 7^{th} iteration of operator T defined in (19) for the maps $w_1(x) = \frac{1}{2}x$ and $w_2(x) = \frac{1}{2}x + \frac{1}{2}$ together with greyscale maps $\phi_1(y) = \frac{2}{5}y + \frac{3}{5}$ and $\phi_2(y) = \frac{4}{5}y + \frac{1}{5}$ starting from $u_0(x) = 12\left(x - \frac{1}{2}\right)^2$, b) its associated cumulative distribution function.

If the assumption of having $N = 2$ wavelets maps, $w_1(x) = \frac{1}{2}x$ and $w_2(x) = \frac{1}{2}x + \frac{1}{2}$, as in the last example is coupled with the same ambiguity aversion for both assessments, $\omega_1 = \omega_2 = \frac{1}{2}$, the greyscale maps' parameters turn out to be $\alpha_1 = \alpha_2 = \frac{\omega_i}{2s_i} = \frac{1}{2}$ and $\beta_1 = \beta_2 = \frac{1-\omega_i}{2s_i} = \frac{1}{2}$, so that operator T, which is still a contraction as $\frac{1}{2}\sum_{i=1}^{2}\omega_i s_i^{-\frac{1}{2}} = 0.71 < 1$, becomes perfectly symmetric. In this case, whenever the initial density u_0 is different than the uniform density, convergence toward the (unique) fixed point, which, by Corollary 3, must be the uniform density $\bar{u}(x) \equiv 1$, becomes smoother than the transition path described in Figure 14(a), where the taller spikes of the finite marginal densities are concentrated toward the right endpoint of the interval $[0, 1]$: Figure 15(a) shows that the 7^{th} iteration of operator T as obtained by running our Maple algorithm starting from the same bimodal initial density $u_0(x) = 12\left(x - \frac{1}{2}\right)^2$. Unlike the marginal density in Figure 14(a) has spikes which are smaller and uniformly distributed over the whole interval $[0, 1]$, while the associated cumulative distribution function reported in Figure 15(b) looks quite the same as that in Figure 14(b). Such a configuration envisages a faster convergence toward the unique fixed point $\bar{u}(x) \equiv 1$.

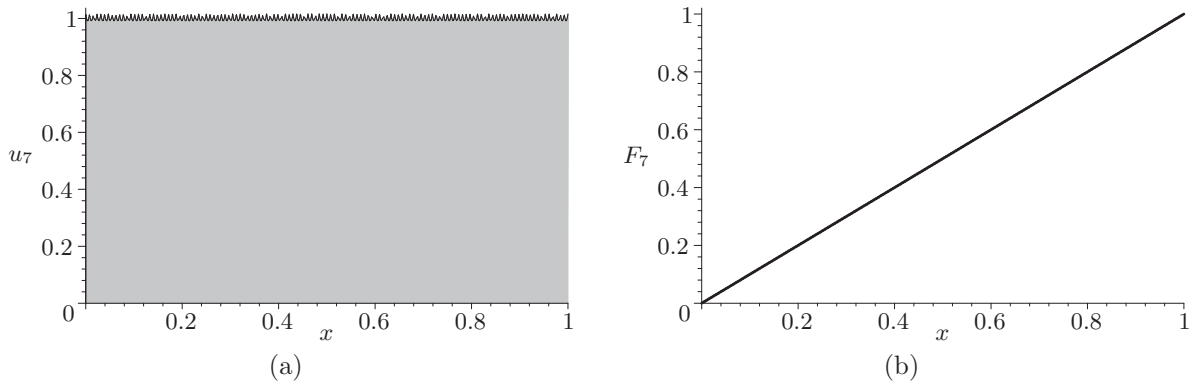

FIGURE 15: a) 7^{th} iteration of operator T defined in (19) for the maps $w_1(x) = \frac{1}{2}x$ and $w_2(x) = \frac{1}{2}x + \frac{1}{2}$ together with greyscale maps $\phi_1(y) = \phi_2(y) = \frac{1}{2}y + \frac{1}{2}$ starting from $u_0(x) = 12\left(x - \frac{1}{2}\right)^2$, b) its associated cumulative distribution function.

The next example recalls the same $N = 3$ assessments considered in Figures 8 and 9 to which ambiguity aversion is being added. Specifically, we set $\gamma = 0.02$, $r_1 = 0.02$, $\tau_1 = 0.8925$ $g_1 = 0$, $\gamma = 0.02$, $r_2 = 0.05$, $\tau_2 = 0.6675$, $g_2 = 0.1275$, and $\gamma = 0.02$, $r_3 = 0.08$, $\tau_3 = 0.57$, $g_3 = 0.51$ so that the maps $w_i(x) = s_i x + a_i$ have parameters $s_1 = \frac{1+r_1-\tau_1}{1+\gamma} = \frac{1}{8}$, $a_1 = \frac{g_1}{1+\gamma} = 0$, $s_2 = \frac{1+r_2-\tau_2}{1+\gamma} = \frac{3}{8}$, $a_2 = \frac{g_2}{1+\gamma} = \frac{1}{8}$ and $s_3 = \frac{1+r_3-\tau_3}{1+\gamma} = \frac{1}{2}$, $a_3 = \frac{g_3}{1+\gamma} = \frac{1}{2}$ respectively. By assuming $\omega_1 = \frac{1}{5}$, $\omega_2 = \frac{2}{5}$ and $\omega_3 = 1$, so that in the third assessment there is no ambiguity aversion, the greyscale maps $\phi_i(y) = \alpha_i y + \beta_i$ have parameters $\alpha_1 = \frac{\omega_1}{3s_1} = \frac{8}{15}$ and $\beta_1 = \frac{1-\omega_1}{3s_1} = \frac{32}{15}$, $\alpha_2 = \frac{\omega_2}{3s_2} = \frac{16}{45}$ and $\beta_2 = \frac{1-\omega_2}{3s_2} = \frac{8}{15}$, $\alpha_3 = \frac{\omega_3}{3s_3} = \frac{2}{3}$ and $\beta_3 = \frac{1-\omega_i}{3s_i} = 0$. Again the operator T defined in (19) satisfies Assumption A.1 and is a contraction as $\frac{1}{2}\sum_{i=1}^{2}\omega_i s_i^{-\frac{1}{2}} = 0.88 < 1$, so that its fixed point exists, is unique and is a density starting form any initial density u_0. Figure 16(a) shows the 5^{th} iteration of operator T as obtained by running our Maple algorithm starting from the uniform initial density $u_0(x) \equiv 1$, while Figure 16(b) reports the corresponding cumulative distribution function.

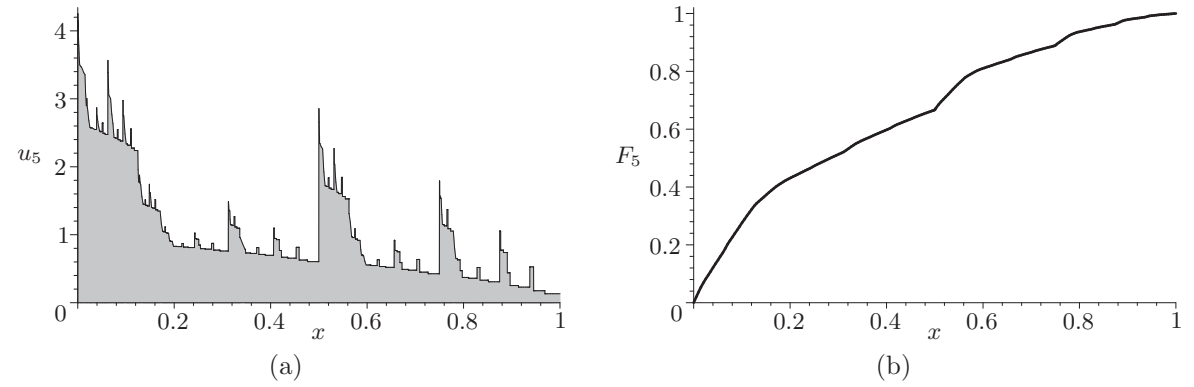

FIGURE 16: a) 5^{th} iteration of operator T defined in (19) for the maps $w_1(x) = \frac{1}{8}x$, $w_2(x) = \frac{3}{8}x + \frac{1}{8}$ and $w_3(x) = \frac{1}{2}x + \frac{1}{2}$ together with greyscale maps $\phi_1(y) = \frac{8}{15}y + \frac{32}{15}$, $\phi_2(y) = \frac{16}{45}y + \frac{8}{15}$ and $\phi_3(y) = \frac{2}{3}y$ starting from $u_0(x) \equiv 1$, b) its associated cumulative distribution function.

Finally, we consider the same $N = 3$ assessments just studied but by exchanging the levels of ambiguity aversion across assessments; that is, to the same maps w_i taken above we set $\omega_1 = \frac{4}{5}$ (low ambiguity aversion) and $\omega_2 = \omega_3 = \frac{1}{10}$ (high ambiguity aversion associated to the last two

assessments),[3] Then, the greyscale maps $\phi_i(y) = \alpha_i y + \beta_i$ have parameters $\alpha_1 = \frac{\omega_1}{3s_1} = \frac{32}{15}$ and $\beta_1 = \frac{1-\omega_1}{3s_1} = \frac{8}{15}$, $\alpha_2 = \frac{\omega_2}{3s_2} = \frac{4}{45}$ and $\beta_2 = \frac{1-\omega_2}{3s_2} = \frac{4}{5}$, $\alpha_3 = \frac{\omega_3}{3s_3} = \frac{1}{15}$ and $\beta_3 = \frac{1-\omega_i}{3s_i} = \frac{3}{5}$. Operator T defined in (19) is a contraction as $\frac{1}{2}\sum_{i=1}^{2}\omega_i s_i^{-\frac{1}{2}} = 0.86 < 1$, and the limit distribution exists, is unique and is a density starting form any initial density u_0. Figure 17(a) reports the 5^{th} iteration of operator T as obtained by running our Maple algorithm starting from the uniform initial density $u_0(x) \equiv 1$, while Figure 17(b) plots the corresponding cumulative distribution function. Now the largest share of ambiguity aversion is attributed to the (last two) maps that are steeper: because they shrink slower horizontally and a larger constant probability is added to them after each iteration, the resulting marginal density after 5 iterations of T in Figure 17(a) turns out to be characterized by a higher spike close to the 0 endpoint and by a flatter pattern on most other points than that in Figure 16(a).

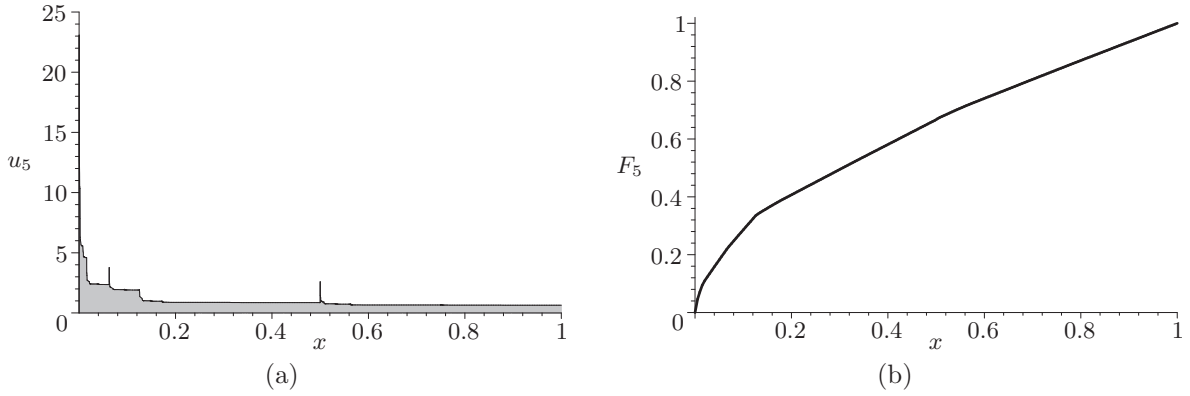

FIGURE 17: a) 5^{th} iteration of operator T defined in (19) for the maps $w_1(x) = \frac{1}{8}x$, $w_2(x) = \frac{3}{8}x + \frac{1}{8}$ and $w_3(x) = \frac{1}{2}x + \frac{1}{2}$ together with greyscale maps $\phi_1(y) = \frac{32}{15}y + \frac{8}{15}$, $\phi_2(y) = \frac{4}{45}y + \frac{4}{5}$ and $\phi_3(y) = \frac{1}{15}y + \frac{3}{5}$ starting from $u_0(x) \equiv 1$, b) its associated cumulative distribution function.

Note that in all examples featuring ambiguity aversion, in order to satisfy the contractivity condition ii) of Proposition 6 the coefficients ω_i must be on average sufficiently small; this requirement becomes stricter as the number N of assessments—*i.e.*, of the maps w_i—increases.

7 Conclusion

Uncertainty is an essential characteristic of macroeconomic dynamics and thus it is important to understand the implications of different sources of uncertainty on economic activities. In the economic growth literature randomness is typically modeled with a scenario-based approach, in which the occurrence of shocks is associated with variables taking on specific values with specific probabilities. However, parameter values are largely unknown and thus this approach does not allow to account for such information-based uncertainty, which instead introduces ambiguity in the picture. Our paper analyze the implications of ambiguity and ambiguity attitude on macroeconomic dynamics by developing a novel approach based on iteration function systems on density functions in the context of economic growth and public debt stabilization. We assume that the debt-to-GDP ratio is described by a random variable to take into account the randomness associated with the formation of expectations, but it is also affected by ambiguity

[3]We cannot use just the opposite levels of the previous case because with $\omega_1 = 1$, $\omega_2 = \frac{2}{5}$ and $\omega_3 = \frac{1}{5}$ the contractivity condition ii) of Proposition 6 would be violated.

since policymakers need to develop subjective assessments to forecast unknown parameter values. We formalize policymakers' response to ambiguity with a simple heuristic rule in which the empirical distribution of the debt ratio is adjusted with an ignorance measure, captured by the uniform distribution. We show that ambiguity is a source of unpredictability since it introduces some singularities in the steady state distribution of the debt ratio. Policymakers' ambiguity aversion removes such an unpredictability by smoothing out the singularities in the steady state distribution reducing thus the degree of uncertainty associated with the equilibrium outcome. However, this comes at the cost of a more uniform and less informative steady state distribution.

We exemplify the implications of our analysis through numerical simulations showing the large variability of the long run outcomes in the debt-to-GDP level. Apart from the cases of convergence to the uniform density characterized by wavelets maps w_i, all our simulations exhibit approximations of the invariant distribution consisting of densities which are decreasing on average, independently of policymakers' ambiguity attitude. Such a property arises not by coincidence: it depends on the choice of having always flatter maps w_i closer to the left endpoint 0 of the interval $[0, 1]$ than those closer to the right endpoint 1. This suggests that the slope of the maps w_i could in principle be tuned by appropriate choices on the policy parameters τ_i and g_i (specifically, by choosing high and zero—or close to zero—values for each of them respectively). In other words, a simple rule of thumb, rather than a sophisticated optimality criterion, on the choice of parameters τ_i and g_i in some assessments may prove effective enough in containing the long-run debt-to-GDP level. It may be interesting thus to analyze how fine-tuning of the policy parameters may lead to long-run distributions which tend to concentrate more mass (probability) on lower values of the debt-to-GDP ratio x_t, providing some level of containment of the public debt from a probabilistic perspective. Extending the analysis along this direction is left for future research.

References

[1] Baker, S.R., Bloom, N., Davis, S.J. (2016). Measuring economic policy uncertainty, Quarterly Journal of Economics 131, 1593—1636

[2] Banach, S. (1922). Sur les opérations dans les ensembles abstraits et leurs applications aux équations intégrales, Fundamenta Mathematicae 3, 133-181.

[3] Barnsley, M. (1989). Fractals Everywhere (Academic Press: New York)

[4] Barnsley, M.F., Ervin, V., Hardin, D., Lancaster, J. (1985). Solution of an inverse problem for fractals and other sets, PNAS 83, 1975–1977.

[5] Barnsley, M., Hurd, L. (1995). Fractal image compression (AK Peters Ltd: Massachusetts)

[6] Born, B., Pfeifer, J. (2014). Policy risk and the business cycle, Journal of Monetary Economics 68, 68—85.

[7] Brainard, W. (1967). Uncertainty and the effectiveness of policy. American Economic Review 57, 411–425

[8] Brock, W., Durlauf, S. (2006). Macroeconomics and model incertainty, in (Colander, D. Ed.), "Post Walrasian macroeconomics: beyond the dynamic stochastic general equilibrium model", 116–134 (Cambridge University Press: Cambridge)

[9] Brock, W.A., Mirman, L.J. (1972). Optimal economic growth and uncertainty: the discounted case, Journal of Economic Theory 4, 479–513.

[10] Camerer, C., Weber, M. (1992). Recent developments in modeling preferences: uncertainty and ambiguity, Journal of Risk and Uncertainty 5, 325–370.

[11] Cozzi, G., Giordani, P.E. (2011). Ambiguity attitude, R&D investments and economic growth, Journal of Evolutionary Economics 21, 303—319.

[12] Elad, M. (2010). Sparse and redundant representations, from theory to applications in signal and image processing (Springer: New York)

[13] Ellsberg, D (1961). Risk, ambiguity and the Savage axioms, Quarterly Journal of Economics 75, 643—669.

[14] Etner, J., Jeleva, M., Tallon, J.M. (2012). Decision theory under ambiguity, Journal of Economic Surveys 26, 234—270.

[15] Forte, B., Vrscay, E.R. (1995). Solving the inverse problem for function and image approximation using iterated function systems, Dynamics of Continuous, Discrete and Impulsive Systems 1, 177–232.

[16] Forte, B., Vrscay, E.R. (1998). Theory of generalized fractal transforms, in (Fisher, Y., Ed.) "Fractal image encoding and analysis", NATO ASI Series F 159, 145–168, (Springer Verlag: New York)

[17] Frisch, D., Baron, J. (1988). Ambiguity and rationality, Journal of Behavioral Decision Making 1, 149–157.

[18] Ghirardato, P., Maccheroni, F., Marinacci, M. (2004). Differentiating ambiguity and ambiguity attitude, Journal of Economic Theory 118, 133—173.

[19] Goldluecke, B., Strekalovskiy, E., Cremers, D. (2012). The natural vectorial total variation which arises from geometric measure theory, SIAM Journal on Imaging Science 5, 537–563.

[20] Hansen, L.P., Sargent, T.J. (2007), Robustness (Princeton University Press: Princeton)

[21] Hutchinson, J. (1981). Fractals and self-similarity, Indiana University Mathematics Journal 30, 713–747.

[22] Kunze, H., La Torre, D., Mendivil, F., Vrscay, E.R. (2012) Fractal-based methods in analysis (Springer: New York)

[23] La Torre, D., Marsiglio, S., Mendivil, F., Privileggi, F. (2015). Self-similar measures in multi-sector endogenous growth models, Chaos, Solitons and Fractals 79, 40–56.

[24] La Torre, D., Marsiglio, S., Privileggi, F. (2018a). Fractal attractors in economic growth models with random pollution externalities, Chaos 28, 055916.

[25] La Torre, D., Marsiglio, S., Mendivil, F., Privileggi, F. (2018b). Fractal attractors and singular invariant measures in two-sector growth models with random factor shares, Communications in Nonlinear Science and Numerical Simulation 58, 185–201.

[26] La Torre, D., Marsiglio, S. (2019). A note on optimal debt reduction policies, Macroeconomic Dynamics, forthcoming

[27] La Torre, D., Vrscay, E.R., Ebrahimi, M., Barnsley, M. (2009), Measure-valued images, associated fractal transforms and the affine self-similarity of images, SIAM Journal on Imaging Science 2, 470–507.

[28] La Torre, D., Mendivil, F., Vrscay, E.R. (2016). Iterated function systems on functions of bounded variations, Fractals 24, 1650019.

[29] Olson, L.J., Roy, S. (2005). Theory of stochastic optimal economic growth, in (Dana, R.A., Le Van, C., Mitra, T., Nishimura, K., Eds.) "Handbook on optimal growth 1: discrete time", 297–336 (Springer: New York)

[30] Rodrik D. (1991), Policy uncertainty and private investment, Journal of Development Economics 36, 229—242.

[31] Rudin, W. (1974). Real and complex analysis (McGraw Hill: New York)

[32] Schauder, J. (1930). Der fixpunktsatz in funktionalräumen, Studia Mathematica 2, 171–180.

[33] Strong, D., Chan, T., (2003). Edge-preserving and scale-dependent properties of total variation regularization, Inverse Problems 19, 165–187.